



Published in final edited form as:

Cell Rep. 2021 March 16; 34(11): 108830. doi:10.1016/j.celrep.2021.108830.

Amino acids-Rab1A-mTORC1 signaling controls whole-body glucose homeostasis

Xin Zhang^{1,2}, Xiaowen Wang^{1,2}, Ziqiang Yuan^{1,3}, Sarah J. Radford¹, Chen Liu⁴, Steven K. Libutti^{1,3}, X.F. Steven Zheng^{1,2,5,*}

¹Rutgers Cancer Institute of New Jersey, Rutgers, The State University of New Jersey, 195 Little Albany Street, New Brunswick, NJ 08901, USA

²Department of Pharmacology, Robert Wood Johnson Medical School, Rutgers, the State University of New Jersey, 675 Hoes Lane, Piscataway, NJ 08854, USA

³Department of Surgery, Robert Wood Johnson Medical School, Rutgers, The State University of New Jersey, 195 Little Albany Street, New Brunswick, NJ 08901, USA

⁴Department of Pathology and Laboratory Medicine, Robert Wood Johnson Medical School, Rutgers, The State University of New Jersey, 195 Little Albany Street, New Brunswick, NJ 08901, USA

⁵Lead contact

SUMMARY

Rab1A is a small GTPase known for its role in vesicular trafficking. Recent evidence indicates that Rab1A is essential for amino acids (aas) sensing and signaling to regulate mTORC1 in normal and cancer cells. However, Rab1A's *in vivo* function in mammals is not known. Here, we report the generation of tamoxifen (TAM)-induced whole body Rab1A knockout (Rab1A^{-/-}) in adult mice. Rab1A^{-/-} mice are viable but become hyperglycemic and glucose intolerant due to impaired insulin transcription and β -cell proliferation and maintenance. Mechanistically, Rab1A mediates AA-mTORC1 signaling, particularly branched chain amino acids (BCAA), to regulate the stability and localization of the insulin transcription factor Pdx1. Collectively, these results reveal a physiological role of aa-Rab1A-mTORC1 signaling in the control of whole-body glucose homeostasis in mammals. Intriguingly, Rab1A expression is reduced in β -cells of type 2 diabetes (T2D) patients, which is correlated with loss of insulin expression, suggesting that Rab1A downregulation contributes to T2D progression.

This is an open access article under the CC BY-NC-ND license (<http://creativecommons.org/licenses/by-nc-nd/4.0/>).

*Correspondence: zhengst@cinj.rutgers.edu.

AUTHOR CONTRIBUTIONS

X.F.S.Z. conceptualized and directed the overall project. X.Z., X.W., and Z.Y. designed and/or performed experiments. C.L. performed mouse tissue pathology analysis. X.Z. prepared figures. X.Z. and X.F.S.Z. wrote the manuscript. X.F.S.Z. and S.K.L. provided funding and research space. X.Z., Z.Y., S.J.R., S.K.L., and X.F.S.Z. edited the manuscript.

DECLARATION OF INTERESTS

The authors declare no competing interests.

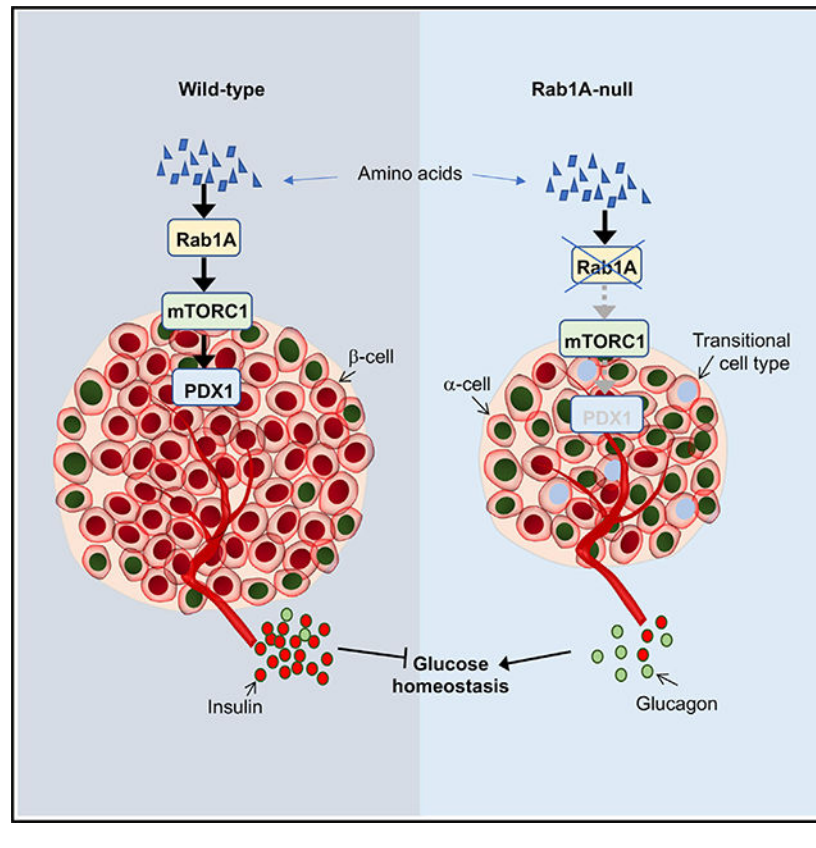
SUPPLEMENTAL INFORMATION

Supplemental Information can be found online at <https://doi.org/10.1016/j.celrep.2021.108830>.

In brief

Zhang et al. generate and analyze inducible Rab1A knockout mice. The results reveal that Rab1A-mTORC1 mediates branched chain amino acids signaling and regulates PDX-dependent insulin transcription and beta-cell trans-differentiation to alpha-cells. This amino acid sensing and signaling mechanism controls whole-body glucose homeostasis in mice and men.

Graphical Abstract



INTRODUCTION

Endoplasmic reticulum (ER) and Golgi apparatus are increasingly recognized as a major hub for cell signaling and regulatory functions in response to extracellular and intracellular cues, particularly nutrient signals (Pahl, 1999; Ron and Walter, 2007). For example, the master lipogenic transcription factors sterol regulatory element binding proteins (SREBPs) are sequestered as an inactive precursor in the ER-Golgi system. In response to nutrient stimulation, SREBPs become proteolytically processed and translocated into the nucleus where they regulate gene expression (Horton et al., 2002; Kim et al., 2008b). Rab1A is a small GTPase that is localized predominantly on the membranes of ER and Golgi apparatus (Plutner et al., 1991; Saraste et al., 1995). Although Rab1 is traditionally known as a component of the intracellular vesicular transport system (Hutagalung and Novick, 2011), recent studies have expanded its function to regulation of mTOR and Notch cell signaling (Charng et al., 2014; Thomas et al., 2014).

Amino acids (aas) are not only nutrients but also mitogenic signals that control cellular growth and metabolism (Jewell et al., 2013; Shimobayashi and Hall, 2016). At the center of aa sensing and signaling is mTORC1, a conserved protein kinase complex and a highly selective protein target of rapamycin (Blenis, 2017; Hara et al., 2002; Hara et al., 1998; Kim et al., 2002; Loewith et al., 2002). Research over the past decade indicates that Rag GTPase is a key mediator of aa signaling to activate mTORC1 (Kim et al., 2008a; Sancak et al., 2008). Rag GTPase heterodimers bind to and recruit mTORC1 to lysosomal membranes, activating mTORC1 through enhanced Rheb-mTORC1 interaction (Sancak et al., 2010) in response to changing lysosomal aa levels (Rebsamen et al., 2015; Wang et al., 2015; Zoncu et al., 2011). Interestingly, aas retain some ability to various degrees in stimulating mTORC1 activity in Rag knockout/knockdown yeast, HEK293 cells, and mouse tissues and cells (Jewell et al., 2015; Stracka et al., 2014; Thomas et al., 2014). These observations indicated that there is an alternative mechanism(s) for aa sensing and signaling. Our subsequent study revealed that Rab1A GTPase mediates aa signaling to activate mTORC1 in a Rag-independent manner in yeast and mammalian cells (Thomas et al., 2014). In contrast to Rag, Rab1A operates through ER/Golgi to activate mTORC1 (Abraham, 2015; Carroll, 2020; Sanchez-Gurmaches and Guertin, 2014; Shimobayashi and Hall, 2016).

Consistent with its growth regulatory functions, Rab1A is widely overexpressed in human diseases such as cancer and cardiomyopathy, contributing to the underlying pathogenesis (Cooper et al., 2006; Wu et al., 2001; Yang et al., 2016). For examples, Rab1A is upregulated in a dilated cardiomyopathy model, and heart-specific Rab1A transgene causes cardiac hypertrophy in a dose- and time-dependent manner (Wu et al., 2001); Rab1A is overexpressed in colorectal cancer, rendering mTORC1 hyperactivation and enhancing cancer cell growth in an aa-dependent manner. Despite the apparent importance of Rab1A in cell biology and diseases, however, Rab1A has not been studied in genetic knockout models in mammals. Here, we report the generation of a tamoxifen-inducible Rab1A knockout mouse model, which unravels a specific role of aa-Rab1A-mTORC1 signaling in insulin transcription and β -cell proliferation and maintenance in adult mice.

RESULTS

Inducible Rab1A knockout in adult mice pancreatic islet-specific defects, hyperglycemia, and glucose intolerance

To explore the physiological function of Rab1A in mammals, we generated unconditional heterozygous Rab1A knockout (Rab1A^{+/-}) mice (C57BL/6J) by deletion of exon 2 of Rab1A genomic locus. Inter-breeding of Rab1A^{+/-} mice failed to produce Rab1A^{-/-} littermates. Rab1A^{-/-} embryos died at ~E10.5–E12.5 due to remarkably smaller embryos, indicating that Rab1A is essential for embryonic growth. This phenotype remarkably similar to that of homozygous RagA knockout embryos (Efeyan et al., 2014), which is consistent with the common function of Rab1A and RagA in aa-mTORC1 signaling. To circumvent the embryonic lethality issue, we constructed a conditional Rab1A allele by floxing exon 2 of Rab1A gene (Rab1A^{Flox/+}) in C57BL/6J mice (Figures 1A and 1B). Cre-ERT2^{+/-}; Rab1A^{Flox/Flox} mice were crossed with R26-CreERT2^{+/-} mice to allow inducible whole-body knockout by tamoxifen (TAM) (Indra et al., 1999). TAM was administered to R26-Cre-

ERT2^{+/-}; Rab1A^{Flox/Flox} and Rab1A^{Flox/Flox} mice at 6 weeks of age. Rab1A was efficiently reduced after 1 week of TAM treatment in major organs including the pancreas, liver, intestines, lung, stomach, bladder, muscle, adipose, heart, and kidney tissues in R26-Cre-ERT2^{+/-}; Rab1A^{Flox/Flox} mice, but not control Rab1A^{Flox/Flox} mice, as judged by immunohistochemistry (IHC) or immunoblot (Figures 1C, 1D, and S1). Rab1A^{-/-} mice were monitored for >2 years post TAM. Rab1A knockout animals were viable and appeared relatively normal, except that they were moderately lighter in body weight than wild-type (WT) mice (Figure 1E).

We next performed histological analysis of Rab1A knockout animals, which showed no apparent abnormality in major tissues except the pancreas. The size increase of pancreatic islets and β -cells with age was attenuated by Rab1A knockout (Figures 2A–2C). In contrast, the number of pancreatic islets remained similar between the two groups (Figure 2D). Ki-67 staining indicated that islet cell proliferation was dampened by Rab1A knockout (Figures 2E and 2F). Strikingly, mTORC1, not mTORC2, signaling was blunted specifically in the pancreas as judged by immunoblot or IHC staining of p-S6/p-S6K/p-4EBP1/p-Ulk1 and p-Akt, respectively (Figures 1C, 1D, and S1). Because β -cell-specific mTORC1 signaling is required for β -cell proliferation (Blandino-Rosano et al., 2017), the growth defect of Rab1A knockout islets is likely due to impaired mTORC1 signaling. Pancreatic islets play a central role in the control of whole-body glucose homeostasis. We therefore examined fasting blood glucose and glucose tolerance. Rab1A^{-/-} mice displayed persistently high fasting blood glucose and were glucose-intolerant (Figures 2G and 2H). However, intraperitoneal administration of insulin induced rapid blood glucose level decrease in both WT and knockout mice (Figure 2I), indicating that insulin sensitivity remained intact. Hence, the hyperglycemic phenotype is likely due to impaired insulin output rather than peripheral insulin resistance.

Rab1A knockout inhibits insulin expression but does not affect insulin secretion in adult pancreatic islets

Because pancreatic islets play a central role in glucose control, we measured circulating insulin after glucose challenge and found that blood insulin level was considerably lower in Rab1A^{-/-} mice than control animals (Figure 3A). To understand the underlying mechanism, we investigated insulin expression in the islets by IHC staining. The result showed that insulin protein content was drastically lower in Rab1A^{-/-} islets (Figures 3B–3E and S2). Although some islets showed uniformed loss of insulin protein expression, other islets had a mosaic phenotype with partial loss of insulin expression (Figure 3B–3E). Both insulin and proinsulin proteins were reduced as revealed by immunofluorescence (IF) staining in mutant mice (Figures 3F and 3G). The reduction in proinsulin protein expression was verified by ELISA assay of isolated Rab1A^{-/-} islets (Figures S3A and S3B). Fluorescence *in situ* hybridization (FISH) and qRT-PCR further revealed reduction of Ins1 and Ins2 mRNA expression (Figures 3H–3J). Hence, genetic ablation of Rab1A impairs insulin mRNA and protein expression in mice.

β -cells sense changes of plasma glucose concentration and release appropriate amounts of insulin from storage to the circulation (Fu et al., 2013). The mutant mice responded rapidly

to glucose challenge in the glucose tolerance test (Figure 2I), suggesting that insulin secretion is not affected. To verify this, we isolated pancreatic islets from 10-week-old Rab1A^{flox/flox}/R26-Cre^{ERT2/-} and Rab1A^{flox/flox}/R26-Cre^{ERT2/+} animals and induced Rab1A knockout with 4-hydroxytamoxifen (Figures S3A and S3B). We next measured glucose stimulation of intracellular Ca²⁺, a key event in regulating insulin exocytosis (Fu et al., 2013). The response of Ca²⁺ flux to glucose was virtually indistinguishable between WT and mutant islets (Figure S3C). Similar results were seen with Rab1A knockdown in the mouse β -cell line MIN6, a common cell model for studying insulin secretion (Figures S3D–S3F). These results suggest that insulin secretion system remains intact. To verify this, we treated MIN6 cells with actinomycin to block glucose stimulation of new insulin biosynthesis (Giddings et al., 1982). Rab1A knockdown reduced insulin release by ~50% (Figure S3G). However, no difference in insulin release was observed after actinomycin treatment between control and Rab1A knockdown cells (Figure S2G), indicating that Rab1A ablation primarily affects insulin biosynthesis rather than secretion.

Rab1A mediates aa regulation of insulin transcription

To investigate the mechanism by which Rab1A regulates insulin expression, we examined insulin expression in murine β -cell lines MIN6 and INS-1 823/13. Rab1A knockdown blunted both Ins1 and Ins2 mRNA expression (Figure 4A), indicating that these cell lines can recapitulate Rab1A's *in vivo* function. Because Rab1A is involved in aa signaling, our finding further raised the possibility that aas regulate insulin expression. Indeed, aa starvation inhibited Ins1 and Ins2 mRNA expression in both MIN6 and INS-1 823/13 cells (Figures 4B and S4A). Rodents carry two insulin genes: the rodent-specific retrogene Ins1 and the human insulin ortholog Ins2 that is the major insulin gene in mice (Soares et al., 1985; Wentworth et al., 1986). Because both insulin genes were similarly regulated, we thereafter focused on the major insulin gene Ins2. Because glucose also controls insulin transcription (Macfarlane et al., 1999; Petersen et al., 1998), we investigated the interplay between aas and glucose on regulation of Ins2. Although both aas and glucose stimulated insulin mRNA expression, glucose's action was dependent on aas (Figure 4C). Knockdown of Rab1A attenuated induction of insulin expression by aas and glucose (Figures 4D, 4E, and S4B). Moreover, rapamycin also blocked aa stimulation of insulin expression (Figure 4F). These results indicate that aas regulates insulin mRNA expression in a Rab1A- and mTORC1-dependent manner.

To investigate how insulin promoter responds to aas, we constructed a firefly luciferase-PEST (Luc) reporter under the control of Ins2 promoter (Figure 4G). The luciferase-PEST reporter enables real-time measurement of promoter activity in living cells (Leclerc et al., 2000; Li et al., 1998), which responded rapidly to aa stimulation (Figure 4H), demonstrating the utility of this reporter in analysis of insulin promoter regulation. We next used the Ins2-Luc reporter to analyze how specific aas regulates insulin transcription. Branched chain amino acids (BCAA, leucine, isoleucine, and arginine), glutamine, and arginine have been implicated in activation of mTORC1 signaling (González and Hall, 2017). Interestingly, all three BCAAs together, rather than each individually, stimulated insulin transcription (Figure 4H). Glutamine or arginine alone was also insufficient to activate insulin transcription (Figure 4H). We next generated contiguous deletions to map Ins2 promoter, which revealed

that -200 to -181 bp was essential for Ins2 promoter response to aas (Figures 4I and 4J). Interestingly, this segment contains an A3 box (TCTAATTA), a conserved Pdx1-responsive element (Melloul et al., 2002). Pdx1 is a major insulin transcription factor (Fujimoto and Polonsky, 2009). Deletion of the A3 box was sufficient to blunt response of Ins2 promoter to aas (Figure 4K), demonstrating that A3 box is required for aa activation of Ins2 promoter.

Rab1A regulates the stability and nuclear localization of Pdx1

Consistent with A3 box is essential for aa response, Pdx1 knockdown blunted aa-induced Ins2 mRNA expression in MIN6 cells (Figure 5A). Pdx1 protein was enriched in the nucleus under normal culture condition, but was decreased drastically in both protein level and nuclear localization on aa starvation (Figures 5B and 5C). Restimulation with full aa or BCAA rapidly restored Pdx1 nuclear localization in an mTORC1- and Rab1A-dependent manner (Figures 5D–5F). We next assessed Pdx1 protein stability in the presence of cycloheximide to block new protein synthesis. The result showed that aa starvation or Rab1A knockdown accelerated Pdx1 degradation (Figures 5G and 5H). Moreover, Pdx1 degradation induced by aa starvation or Rab1A knockdown was suppressed by the proteasomal inhibitor MG132 (Figure 5I). In contrast, Pdx1 mRNA expression was not affected by different conditions (Figures S5A–S5D). Amino acids and glucose cooperate in the regulation of Pdx1 protein stability in a Rab1A-dependent manner (Figure 5J). Consistently, immunoblot and IHC analysis showed considerably reduced Pdx1 protein level in Rab1A^{-/-} islets compared with Rab1A^{+/+} pancreas (Figure 5K). In fact, the majority of the cells were Pdx1⁺ in WT islets but were Pdx1⁻ in Rab1A^{-/-} islets (Figure 5L). On the other hand, Pdx1 showed higher nuclear level under aa starvation in cells overexpressing Flag-Rab1A (Figure S5E). Together, these results showed that aas promotes the stability and nuclear localization of Pdx1 protein in a Rab1A-dependent manner.

Rab1A and aa signaling regulates *trans*-differentiation of β -cells to α -cells

Insulin-producing β -cells and glucagon-producing α -cells are two major pancreatic endocrine cell types. Because insulin⁻ cells were markedly increased in Rab1A^{-/-} mice, we asked if Rab1A knockout affects the identity of islet cells. β -cells normally represent majority of the interior cell population, whereas α -cells are primarily found in the periphery of WT islets (Figures 6A; Xin et al., 2016a). However, β -cell population (insulin⁺glucagon⁻) was dramatically decreased in both absolute numbers and percentage of the islet cells in Rab1A^{-/-} islets (Figures 6B, 6C, and S6A). There was a concomitant increase in glucagon⁺ cells in absolute numbers (>2-fold) and in percentage (>3-fold) (Figures 6C and S6A). Moreover, a majority of glucagon⁺ cells were occupied in the interior of mutant islets (Figure 6B), compared with their normal peripheral localization in WT islets. Interestingly, insulin⁻glucagon⁻ and insulin⁺glucagon⁺ cells were each also increased ~4-fold (Figures 6B, 6C, and S6A). These observations suggest that β -cells underwent *trans*-differentiation to α cells with insulin⁺glucagon⁺ cells likely to be in the transitional stage. Consistently, Pdx1 expression was greatly reduced in Rab1A^{-/-} islets (Figures S6B–S6E). The mature β -cell marker, Ucn3 (Blum et al., 2012), was also diminished in Rab1A^{-/-} islet cells (Figures 6D and 6E). These results indicate that Rab1A knockout results in loss of functional maturity in β -cells. To ask whether the effect of Rab1A knockout on β -cell identity is cell-autonomous, we knocked down Rab1A in MIN6 cells and stained them with glucagon and MafB, a

mature α -cell marker (Artner et al., 2006). MIN6 cells became glucagon⁺ and MafB⁺ after Rab1A downregulation (Figures 6F and 6G), indicating that Rab1A regulates *trans*-differentiation from β -cells to α -cells in a cell-autonomous manner. Finally, in contrast to the decrease of blood glucagon in response to glucose challenge in WT mice, the circulating glucagon level was higher in Rab1A^{-/-} animals that were unresponsive to glucose challenge (Figure 6H). Therefore, Rab1A knockout leads to impaired blood glucagon control.

Rab1A expression is downregulated in β -cells from type 2 diabetes (T2D) patients, which is correlated with loss of insulin expression

A hallmark of T2D is insulin resistance in peripheral tissues, resulting in hyperglycemia, which in turn impairs β -cell proliferation and insulin output (Muio and Newgard, 2008). Transcriptome analysis revealed that insulin mRNA expression is significantly downregulated in T2DM islets (Dominguez et al., 2011; Ma and Zheng, 2018; Segerstolpe et al., 2016). Because Rab1A regulates insulin transcription, we asked if Rab1A expression is altered in T2D by analyzing a transcriptome dataset from human healthy and T2D islets (Dominguez et al., 2011). Rab1A and insulin mRNA was found to be markedly reduced in T2D islets compared with healthy ones (Figures 7A and 7B). Rab1A protein expression, rather than Rab1A GTP-binding, was found to be reduced in the isolated islets from a Western diet (WD)-induced T2D mouse model (Wang and Liao, 2012), compared with control healthy islets (Figures S7A and S7B). Moreover, there was a significant correlation between Rab1A and insulin mRNA expression (Figure 7C). Recent advances in single-cell RNA sequencing (scRNA-seq) make it possible to study gene expression in individual cells. Analysis of a recent scRNA-seq dataset of human non-diabetic (ND) and T2D β -cells (Lawlor et al., 2017) showed that Rab1A and insulin mRNAs were downregulated in the same T2DM β -cells (Figures 7D and 7E). Consistent with the whole islet transcriptome result, Rab1A and insulin mRNA expression was correlated with each other at the single-cell level (Figure 7F). In contrast, expression of glucagon mRNA was increased in T2D β -cells (Figure S7C). These results show that decreased Rab1A expression is a common feature T2DM, which may contribute to the downregulation of insulin biosynthesis during disease progression.

DISCUSSION

In this study, we investigated the physiological function of Rab1A using TAM-inducible Rab1A knockout in adult mice. Our results reveal a pancreatic β -cell-specific function of Rab1A in the control of whole-body glucose homeostasis through multiple mechanisms. First, Rab1A regulates insulin biosynthesis through regulation of insulin transcription. Mechanistically, Rab1A mediates aas, particularly BCAA, signaling to regulate Pdx1 protein stability and nuclear localization in an mTORC1-dependent manner (see Figure 7G for a working model). Because Rag GTPases are also a major mediator of aa signaling to activate mTORC1, we further investigated their role in insulin transcription. The results show that RagA/B knockdown also inhibits Pdx1 stability and nuclear accumulation and attenuates aa induction of insulin expression (Figures S7D–S7G). Interestingly, although Rab1A has been implicated in insulin trafficking or maturation (Liu et al., 2016; Zhang et al., 2019), Rab1A knockout does not affect glucose stimulation of Ca²⁺ flux and insulin release, suggesting

that Rab1A is not essential for these processes under normal *in vivo* physiological condition. Our study is also consistent with a recent finding that aa-mTORC1 signaling regulates insulin secretion during embryonic development but not in mature β -cells after birth (Helman et al., 2020). Second, loss of Rab1A results in massive loss of β -cell identity to insulin⁻glucagon⁻ cells and to α -cells due to *trans*-differentiation. The latter results in dysregulation of circulating glucagon, which may further contribute to the hyperglycemic phenotype. Of note, a previous study in human T2D patients did not observe a significant increase in absolute number of α -cells (Henquin and Rahier, 2011). It remains to be further determined if the *trans*-differentiation from β -cells to α -cells also occur in human T2D patients. Finally, Rab1A is required for β -cell proliferation, and Rab1A knockout attenuates the increase in islet size and β -cell mass during young adulthood, which is likely to be due to dampened mTORC1 signaling, which is known to be required for β -cell proliferation in mice (Blandino-Rosano et al., 2017).

Mammals tightly maintain whole body glucose homeostasis through endocrine α and β cells (Röder et al., 2016). During fasting when circulating glucose level is low, glucagon is released from α cells that stimulates the conversion of liver glycogen to glucose and increases blood glucose. After meal when circulating glucose is high, insulin is released from β cells to promote uptake and utilization of glucose in peripheral tissues and lower circulating glucose. Many studies have shown that aas also affect circulating insulin level (Newsholme et al., 2007). Protein diet increases plasma insulin concentration in both healthy and T2D human subjects (Pallotta and Kennedy, 1968; Rabinowitz et al., 1966). Intravenous infusion of free aas, particularly BCAA, similarly improves glucose level in T2D patients (Floyd et al., 1966, 1968). Moreover, aas stimulate insulin secretion in isolated human and rodent pancreatic islets and β -cell lines (Newsholme et al., 2007). Our data indicate that enhancing insulin biosynthesis rather than release is the primary mechanism for aas to control insulin output. Interestingly, glucose stimulates insulin transcription much more potently in the presence of aas, suggesting that there is a synergistic action in the two major nutrients in regulating insulin biosynthesis.

Diabetes is a metabolic disease characterized by chronic hyperglycemia due to loss of β -cells and defective insulin release (type 1 diabetes [T1D]), insulin resistance in peripheral tissues (T2D), or both (Kharroubi and Darwish, 2015). T2D starts from insulin resistance in peripheral tissues, resulting in moderate hyperglycemia. The latter leads to “glucose toxicity” that in turn further impairs β -cell proliferation and insulin output capacity. It creates a “vicious cycle” that leads to further deterioration of β -cells (Ebrahimi et al., 2020; Jonas et al., 1999) and progressive loss in insulin biosynthetic capacity (Muioio and Newgard, 2008). T2D conditions promote degradation of Pdx1 protein in a proteasome-dependent manner (Boucher et al., 2006; Harmon et al., 2005). Our data show that Rab1A expression is significantly reduced in β cells of T2D patients, which is correlated with loss of insulin expression. Because Rab1A is required for Pdx1 stability, downregulation of Rab1A may contribute to the progression of T2D. Further studying the role of Rab1A in the control of pancreatic endocrine hormones should help better understand the pathobiology and improve the management of diabetes.

STAR★METHODS

RESOURCE AVAILABILITY

Lead contact—Further information and requests for resources and reagents should be directed to and will be fulfilled by the Lead Contact, Dr. X.F. Steven Zheng (zhengst@cinj.rutgers.edu)

Materials availability—All unique/stable reagents generated in this study are available from the Lead Contact with a completed Materials Transfer Agreement.

Data and code availability statement—This study did not generate any unique datasets or code. Original data is available here: <http://data.mendeley.com/login?redirectPath=/datasets/hd3tvf2twr/draft?a=86069216-4c1c-444f-a681-53d9eb4a083c>

EXPERIMENTAL MODEL AND SUBJECT DETAILS

Animal—All animal care and treatments were carried out in compliance with Rutgers University Institutional Animal Care and Use Committee (IACUC) guidelines. *Rab1A^{Flox/+}* mice were generated by Biocytogen in the C57BL/6J background by floxing exon 2 of *Rab1A* allele (<https://biocytogen.com/gene-editing/by-strategies/#conditional-knockout>). *Rab1A^{Flox/+}* mice were screened and verified by PCR and Southern blot analysis, and confirmed by long-PCR sequencing. *Rab1A^{Flox/Flox}* mice were then mated with *ROSA-Cre^{ERT2/ERT2}* (Ventura et al., 2007) to generate *ROSA-Cre^{ERT2/+}; Rab1A^{Flox/+}* mice. *ROSA-Cre^{ERT2/+}; Rab1A^{Flox/+}* mice were further backcrossed to generate *ROSA-Cre^{ERT2/+}; Rab1A^{Flox/Flox}* mice. Genotyping was performed by PCR analysis of tail DNA. Tamoxifen (TAM) was suspended at a concentration of 20 mg/ml in a mixture of 98% sunflower seed oil and 2% ethanol. 200 μ l TAM per 25 g of body weight was injected intraperitoneally into 8–10-week-old *ROSA-Cre^{ERT2/+}; Rab1A^{Flox/Flox}* and the control *Rab1A^{Flox/Flox}* mice once per day for 5 consecutive days to generate cohorts of *Rab1A* (*Rab1A^{-/-}*) and wild-type control mice (*Rab1A^{+/+}*). To assess *Rab1A* knockout efficiency post TAM, mice were dissected and major organs (pancreas, kidney, liver, intestine, colon, stomach, heart, lung and brain) were collected and analyzed by qRT-PCR and immunoblot for mRNA and protein expression, respectively. For phospho-S6(S240/244) staining in tissues, both control and *Rab1A* KO mice were fasted for overnight (~12 h) and re-fed with normal chow for 2 h. The mice were then sacrificed and proceeded for immunohistochemical analysis. Both male and female mice were used in this study.

Pancreatic β -cell lines—Low passage rat insulinoma cell line INS-1 823/13 and mouse insulinoma cell line MIN6 cells were obtained from Dr. Sally Radovick (Rutgers Robert Wood Johnson Medical School). INS-1 823/13 cells were cultured in RPMI1640 (GIBCO, 72400–047) with 10% fetal bovine serum (FBS). MIN6 were routinely maintained in Dulbecco's modified Eagle's medium (DMEM, GIBCO, 10566–016) with 25 mM glucose, supplemented with 15% FBS and 50 μ M 2-mercaptoethanol. INS-1 823/13 and MIN6 cells presented in this study were at passages less than 30 in a humidified atmosphere with 5% CO₂ at 37°C. All assays used cells with 80% confluence unless otherwise indicated.

METHOD DETAILS

Reverse transcription and Quantitative PCR—Total RNA was isolated from cells or tissues using TRIzol reagent (Thermo Fisher) according to manufacturer's instruction. cDNA synthesis was conducted using GoScript reverse transcription system (Promega) per manufacturer's instructions. Quantitative PCR was performed with SYBR Green PCR master mix (Applied Biosystems) using ViiA 7 Real-Time PCR System (Applied Biosystems). β -actin was used as the internal control. Data were normalized by using the average C_t value of the internal control and further analyzed by the 2^{-C_t} method.

Cell cultures—INS-1 823/13 were cultured in RPMI-1640 (GIBCO, 72400–047) with 10% fetal bovine serum (FBS). MIN6 were maintained in DMEM (GIBCO, 10566–016) with 25mM glucose, supplemented with 15% FBS and 50 μ M 2-mercaptoethanol. Cells in different assays were typically grown to 80% confluence unless otherwise indicated AA starvation and stimulation were conducted as described previously (Thomas et al., 2014). Briefly, cells were rinsed twice with PBS and incubated in RPMI-1640 without AAs supplemented with high glucose (GIBCO, A2494001) and 15% dialyzed FBS (GIBCO, A3382001) for indicated time. 10x AA mixture in the above medium were added for indicated times. Cell samples were analyzed by quantitative PCR, IF or luciferase assay using the Renilla Luciferase Assay System (Promega). The specific amino acids mixture was prepared from individual amino acid powders. Concentrations of used amino acids: leucine, 200 μ M., isoleucine, 100 μ M., valine, 230 μ M., arginine, 50 μ M., glutamine, 2 mM. All the amino acids were purchased from sigma Aldrich as described in the STAR methods.

Plasmids, shRNA, lentivirus production and stable cell lines—The Rapid Response™ luciferase pGL4.84 vector was purchased from Promega (Cat#: E7521). The PX458 vector was obtained from Addgene (Cat #: 48138). The 500 bp mouse *Insulin 2* promoter (*Ins2*) DNA sequence was amplified by PCR, verified by direct DNA sequencing, and inserted into pGL4.84 to generate pGL4.84-*Ins2*. Serial deletions of *Ins2* promoter were generated from pGL4.84-*Ins2* using the QuickChange site-directed Mutagenesis Kit (Agilent Stratagene). Stable cell lines were established with pGL4.84-*Ins2* and *Ins2* deletion plasmids. Plasmid DNA was transfected into MIN6 cells and selected by puromycin (GIBCO) at 0.5 μ g/ml for 3 weeks. Single clones were obtained by serial dilution. Lipofectamine 3000 (Invitrogen) was used for plasmid DNA transfection, while RNAiMAX (Invitrogen) was used for siRNA transfection, according to the manufacturer's instructions. Cells were transfected with 50 nM siRNA for 60 h unless otherwise stated. Mouse *Rab1A* siRNAs were purchased from GenePharma. Mouse *mTOR* siRNAs were purchased from Dharmacon-Thermo Scientific (siGENOME mouse Mtor, MU-065427–00–0002). Mouse *Pdx1* siRNA were designed as described previously (Babu et al., 2008) and synthesized by GenePharma or purchased from Sigma esiRNA (EMU046321).

Mouse Rab1A shRNAs were purchased in GenePharma (Shanghai, China). Four targets against Rab1A mRNA sequence were shown here. shRab1A #1: GGTGGAAAGTCCTGCCTTCT; shRab1A #2: GCACAATTGGTGTGGATTCA; shRab1A #3: GGAGTCCTTCAATAACGTAA; shRab1A #4: GCAACGAATGTAGAACAGTCT. The lentivirus was prepared as the manual instructed

(Genepharma). Briefly, the transfer plasmid pGLV-H1-GFP&Puro-shRab1A (1 μ g) was mixed with packaging plasmids pRSV-Rev (3.75 μ g), pMDLg/pRRE (3.75 μ g) and pCMV-VSV-G (2 μ g) together using Lipofectamine 3000. The plasmids mixture was added to the 70% confluent 293T cell in 10cm dish. The lentivirus was harvested and enriched at 60 hours post transfection. The transfected MIN6 cells were selected by puromycin at 0.5mg/mL and then sorted by FACS for stable cell line establishment. TRC lentiviral shRNAs targeting RagA, RagB in mouse were obtained from Sigma. The TRC number for each shRNA is as shown in the Key resources table. Mouse RagA shRNA #1: TRCN0000337548; Mouse RagA shRNA #2: TRCN0000311262; Mouse RagB shRNA #1: TRCN0000102658; Mouse RagB shRNA #2: TRCN0000102656. shRNA-encoding plasmids were co-transfected with co-transfected with Delta VPR envelope and CMV VSV-G packaging plasmids into actively growing HEK293T cells using FuGENE 6 transfection reagent.

Immunological reagents and immunoblot—See Key resources table for antibodies used against mouse RAB1A, p-S6K1(Thr389), S6K1, p-4E-BP1(Thr37/46), 4E-BP1, p-AKT(Ser473), AKT, Ki-67, Insulin, GM130, Proinsulin, PDX1, NeuroD1, mTOR, Glucagon, β -actin, anti-rabbit horseradish peroxidase (HRP)-conjugated secondary antibodies, anti-mouse HRP-conjugated secondary antibodies, anti-goat HRP-conjugated secondary antibodies. Primary antibodies were used according to manufacturers' instructions overnight at 4°C unless otherwise indicated. Secondary antibodies were used at a dilution of 1:5,000 for 1 h at room temperature. Immunoblot was carried out as described previously (Li et al., 2006; Wei et al., 2009; Zhang et al., 2015). Briefly, cell and tissue protein extracts were separated by SDS-polyacrylamide gel electrophoresis (PAGE) and were transferred onto PVDF membranes (Bio-Rad). Membranes were blocked with 5% skim milk for 1 h at room temperature, and then incubated in primary antibodies overnight at 4°C. Antibodies were diluted according to the manufacturer's instructions. Membranes were further incubated with HRP-conjugated secondary antibodies, followed with enhanced chemiluminescence detection reagents (NEL105001EA, Perkin Elmer) and analyzed using the ChemiDoc XRS+ system (Bio-Rad). Data were quantified using the Image Laboratory v.6.0.1 Software.

Histology and immunohistochemistry—Tissue staining was carried out as previously described with slight modifications (Tsang et al., 2018; Wu et al., 2015; Zhang et al., 2018). Mouse tissues were fixed in 10% neutral buffered formalin solution (Sigma, HT501640) overnight. Fixed tissues were transferred to 75% ethanol and then embedded in paraffin. For frozen sections, tissues were fixed in 10% neutral buffered formalin solution overnight, transferred into 15% sucrose until sinking, and then placed in 30% sucrose overnight. For immunofluorescence (IF) staining, cells or tissue sections were fixed for 10 min with 4% paraformaldehyde (PFA, Sigma), permeabilized with ice cold 0.05% Triton X-100 in PBS and incubated with primary antibodies in 5% normal donkey serum for 1 h at room temperature or overnight at 4°C, followed by incubation with fluorophore-conjugated secondary antibodies. The concentrations of the primary and secondary antibodies are shown below. The mounting medium was obtained from Molecular Probes. Images were captured with Nikon A1R laser scanning confocal microscope. RNA FISH was performed in mouse

pancreatic tissues using Stellaris RNA-FISH complex probe sets (Bio-search Technologies) according to the manufacturer's protocol. The mouse Insulin1/2 probe sets were customized, and Quasar 570-labeled. Pancreas were dissected and processed uniformly. Around one fifth of the pancreas (same or similar position) was cut, embedded in OCT compound (Tissue-Tek® by Sakura) and frozen at -80°C for cryosectioning. $8\ \mu\text{m}$ thick sections were cut using a cryostat. HE staining was performed as described previously (Fischer et al., 2008). Islets areas were determined by ImageJ software as described (Fu et al., 2009; Granot et al., 2009). For β cell size evaluation, the size of the islet area was divided by the number of β cells of the islet as described (Fu et al., 2009). Tissue sections were examined separately by three independent investigators in a blinded fashion.

Metabolic studies—Metabolic studies were performed according to the recommendations of the Mouse Metabolic Phenotyping Center (MMPC) Consortium (Ayala et al., 2010). Body weight and blood glucose of *Rab1A* knockout and control mice were monitored monthly post TAM. Mice were fasted for 6 h (morning fast) and blood glucose was evaluated with a glucometer (MEDSOURCE). Mice were then weighed and injected with glucose intraperitoneally at 2 mg/g body weight. Blood glucose level was measured every 30 min. For the insulin tolerance test, mice were fasted for 4 h and then injected intraperitoneally with insulin at 0.75 U/kg body weight. Blood glucose levels were measured at indicated times. For *in vivo* insulin or glucagon measurements, blood was collected from the tail vein prior to, and 5 minutes and 30 minutes after intraperitoneal injection with glucose (2 mg/g body weight). Blood samples were centrifuged, and serum was collected and measured for insulin concentration using the Insulin ELISA kit (Merckodia).

Circulating insulin and glucagon—For *in vivo* circulating insulin measurement, blood was collected from the tail vein at 30 min after intraperitoneal injection of glucose (2 g/kg body weight). Blood samples were centrifuged, and serum was collected for the measurement of insulin concentrations using the Insulin ELISA kit (Merckodia, #10–1247-01) following manufacturer's instructions. For circulating glucagon measurement, serum was collected from the tail vein from mice fasted overnight or mice at 30 min post glucose challenge (I.P. 2 g/kg body weight). Glucagon was measured using Rodent glucagon ELISA kit (Merckodia, #10–1281-01).

Islets isolation—Islets were isolated from 10-week-old female and male mice as previously described (Carter et al., 2009). After overnight recovery, islets were hand-picked and transferred to RPMI media containing 11.1 mM glucose supplemented with 10% heat-inactivated fetal bovine serum (Biowest, France) and 1% Penicillin-Streptomycin (GIBCO).

Glucose stimulated insulin secretion (GSIS) and calcium influx assays—For GSIS assays, MIN6 cells were initially seeded into 96 well plates in high glucose DMEM media 12 h before experiments. *Rab1A* siRNA and controls were transfected using lipofectamine 3000. In the meantime, Actinomycin D (Sigma Aldrich, A9415) or DMSO as control were added into at 1 $\mu\text{g}/\text{mL}$. 12 h later, the cells were proceeded for GSIS assay as described elsewhere. Briefly, cells were pre-incubated with DMEM media (no FBS, no glucose) for 2 h. Then the cells were incubated with DMEM media containing 1mM

glucose. After incubation for 30 min, the cells were incubated with DMEM media containing 3 mM or 20 mM glucose for 1 h (basal: 3 mM; stimulatory: 20 mM). The supernatant from different wells was collected for further ELISA analysis (Mercodia Rat/Mouse ELISA, Sweden).

For calcium influx measurements, experiments were performed in size-matched isolated pancreatic islets or control/Rab1A knockdown MIN6 cells. Briefly, 8 islets of 150–200 μm diameter or MIN6 cells kept in 96-well plates were pre-incubated for 1 h in Krebs-Ringer bicarbonate (KRB) buffer containing (in mM): 120 mM NaCl, 5 mM KCl, 1 mM MgCl_2 , 2.5 mM CaCl_2 , 25 mM NaHCO_3 supplemented with 0.5% bovine serum albumin and 1 mM glucose. Islets or Cells were loaded with the Ca^{2+} -sensitive dye Fluo-4 followed manufacturer's instructions (Fluo-4 Direct Calcium Assay Kit, F10471, Thermo Fisher). After incubation for calcium dye loading, the calcium signal from 1 mM glucose KRB buffer was measured as the basal value. Then, the islets or cells were transferred to KRB buffer with 20 mM glucose and 0.5% BSA. The calcium influx was measured using Tecan Infinite M200 microreader (Tecan Trading, model: Infinite M200) as previously described (Martínez et al., 2017). The data was calculated using the average of first 9 cycles (unstimulated) as baseline.

Proinsulin ELISA quantification—Proinsulin contents from 10 size-matched Islets and same amount of MIN6 cells (shcontrol and shRab1A) were obtained by acid-ethanol extraction as described elsewhere. Proinsulin concentrations were determined using the Insulin Rat/Mouse Proinsulin ELISA kit from Mercodia (10–1232-01, Sweden).

GEO Datasets Analysis—The GSE datasets (GSE25724, 86469 and 81608) were obtained from GEO website. The genes were annotated and analyzed by R studio. Insulin, Rab1A, Pdx1 and glucagon expression levels of non-diabetic and diabetic groups were plotted using Graph prism.

GTP-binding assay—We performed the GTP-binding assay of Rab1A as previously described (Thomas et al., 2014). Briefly, islets from normal chow and western diet fed mice were dispersed by 0.25% Trypsin, then protein was harvested and suspended in binding buffer (20 mM HEPES pH 8, 150 nM NaCl, 10 mM MgCl_2 , 5x Roche Protease Cocktail Inhibitor Complete) and lysed using three freeze thaw cycles. The cell lysates were centrifuged at 14,000x g and the supernatants were incubated with 100 μl of GTP-Agarose suspension for 1 hr with rotation at 4°C. The beads were collected and washed three times in binding buffer and suspended in 50 μl SDS-PAGE sample buffer for western blot analysis.

Western diet (WD)-induced T2D mouse model—WD-induced T2D mouse model was established as described (Wang and Liao, 2012). Eight-week-old male mice were injected with tamoxifen to induce Rab1A knockout as above described. One week later the mice were fed *ad libitum* for 16 weeks on either a standard chow (7% fat control diet, TD.170522, ENVIGO) or a western diet (5%kcal Fat Diet, TD.08811, ENVIGO). Glucose and insulin tolerance tests were conducted to verify hyperglycemia induced by WD. The mice were sacrificed at 24 weeks for islets collection.

QUANTIFICATION AND STATISTICAL ANALYSIS

Significance levels for comparisons between groups were determined with unpaired two-tailed Student's t test using GraphPad Prism v.7 software or Excel (Microsoft Office) unless specified otherwise. All data were expressed as means \pm standard error of the mean (s.e.m). $p < 0.05$ were considered statistically significant. Samples size was chosen in advance on the basis of common practice of the described experiment and is indicated for each experiment. Experiments were appropriately randomized. Investigators were not blinded during the experiments and outcome assessment unless otherwise stated. Each experiment was conducted with biological replicates and repeated multiple times (3). The statistical parameters are specified within the figure legends.

Supplementary Material

Refer to Web version on PubMed Central for supplementary material.

ACKNOWLEDGMENTS

We thank Dr. Fred Wondisford for discussions, Sally Radovick for providing MIN6 and INS-1 823/13 cell lines, Dr. Wenjin Chen for help with tissue imaging, Ms. Xin Chen for help with animal care, and Ms. Xiaofan Tian for assistance with Ins2-Luc reporter analysis. RCINJ Advanced Microscopy, Biomedical Informatics, Biospecimen Repository, and Flow Cytometry/Cell Sorting and Genome Editing Shared Resources were supported by United States National Institutes of Health (P30 CA072720). This work was supported by United States National Institutes of Health (R01 DK124897 to X.F.S.Z.).

REFERENCES

- Abraham RT (2015). Cell biology. Making sense of amino acid sensing. *Science* 347, 128–129. [PubMed: 25574008]
- Artner I, Le Lay J, Hang Y, Elghazi L, Schisler JC, Henderson E, Sosa-Pineda B, and Stein R (2006). MafB: an activator of the glucagon gene expressed in developing islet alpha- and beta-cells. *Diabetes* 55, 297–304. [PubMed: 16443760]
- Ayala JE, Samuel VT, Morton GJ, Obici S, Croniger CM, Shulman GI, Wasserman DH, and McGuinness OP; NIH Mouse Metabolic Phenotyping Center Consortium (2010). Standard operating procedures for describing and performing metabolic tests of glucose homeostasis in mice. *Dis. Model. Mech* 3, 525–534. [PubMed: 20713647]
- Babu DA, Chakrabarti SK, Garmey JC, and Mirmira RG (2008). Pdx1 and BETA2/NeuroD1 participate in a transcriptional complex that mediates short-range DNA looping at the insulin gene. *J. Biol. Chem* 283, 8164–8172. [PubMed: 18252719]
- Blandino-Rosano M, Barbaresso R, Jimenez-Palomares M, Bozadjieva N, Werneck-de-Castro JP, Hatanaka M, Mirmira RG, Sonenberg N, Liu M, Rüegg MA, et al. (2017). Loss of mTORC1 signalling impairs β -cell homeostasis and insulin processing. *Nat. Commun* 8, 16014. [PubMed: 28699639]
- Blenis J (2017). TOR, the Gateway to Cellular Metabolism, Cell Growth, and Disease. *Cell* 171, 10–13. [PubMed: 28888322]
- Blum B, Hrvatin S, Schuetz C, Bonal C, Reznia A, and Melton DA (2012). Functional beta-cell maturation is marked by an increased glucose threshold and by expression of urocortin 3. *Nat. Biotechnol* 30, 261–264. [PubMed: 22371083]
- Boucher M-J, Selander L, Carlsson L, and Edlund H (2006). Phosphorylation marks IPF1/PDX1 protein for degradation by glycogen synthase kinase 3-dependent mechanisms. *J. Biol. Chem* 281, 6395–6403. [PubMed: 16407209]
- Carroll B (2020). Spatial regulation of mTORC1 signalling: Beyond the Rag GTPases. *Semin. Cell Dev. Biol.* 107, 103–111. [PubMed: 32122730]

- Carter JD, Dula SB, Corbin KL, Wu R, and Nunemaker CS (2009). A practical guide to rodent islet isolation and assessment. *Biol. Proced. Online* 11, 3–31. [PubMed: 19957062]
- Chang WL, Yamamoto S, Jaiswal M, Bayat V, Xiong B, Zhang K, Sandoval H, David G, Gibbs S, Lu HC, et al. (2014). *Drosophila* Tempura, a novel protein prenyltransferase α subunit, regulates notch signaling via Rab1 and Rab11. *PLoS Biol.* 12, e1001777. [PubMed: 24492843]
- Cooper AA, Gitler AD, Cashikar A, Haynes CM, Hill KJ, Bhullar B, Liu K, Xu K, Strathearn KE, Liu F, et al. (2006). α -synuclein blocks ER-Golgi traffic and Rab1 rescues neuron loss in Parkinson's models. *Science* 313, 324–328. [PubMed: 16794039]
- Dominguez V, Raimondi C, Somanath S, Bugliani M, Loder MK, Edling CE, Divecha N, da Silva-Xavier G, Marselli L, Persaud SJ, et al. (2011). Class II phosphoinositide 3-kinase regulates exocytosis of insulin granules in pancreatic beta cells. *J. Biol. Chem* 286, 4216–4225. [PubMed: 21127054]
- Ebrahimi AG, Hollister-Lock J, Sullivan BA, Tsuchida R, Bonner-Weir S, and Weir GC (2020). Beta cell identity changes with mild hyperglycemia: Implications for function, growth, and vulnerability. *Mol. Metab* 35, 100959. [PubMed: 32244186]
- Efeyan A, Schweitzer LD, Bilate AM, Chang S, Kirak O, Lamming DW, and Sabatini DM (2014). RagA, but not RagB, is essential for embryonic development and adult mice. *Dev. Cell* 29, 321–329. [PubMed: 24768164]
- Fischer AH, Jacobson KA, Rose J, and Zeller R (2008). Hematoxylin and eosin staining of tissue and cell sections. *CSH Prot* 2008, pdb.prot4986.
- Floyd JC Jr., Fajans SS, Conn JW, Knopf RF, and Rull J (1966). Stimulation of insulin secretion by amino acids. *J. Clin. Invest* 45, 1487–1502. [PubMed: 5919350]
- Floyd JC Jr., Fajans SS, Conn JW, Thiffault C, Knopf RF, and Guntzsch E (1968). Secretion of insulin induced by amino acids and glucose in diabetes mellitus. *J. Clin. Endocrinol. Metab* 28, 266–276. [PubMed: 4865756]
- Fu A, Ng AC, Depatie C, Wijesekara N, He Y, Wang GS, Bardeesy N, Scott FW, Touyz RM, Wheeler MB, and Sreanor RA (2009). Loss of Lkb1 in adult beta cells increases beta cell mass and enhances glucose tolerance in mice. *Cell Metab.* 10, 285–295. [PubMed: 19808021]
- Fu Z, Gilbert ER, and Liu D (2013). Regulation of insulin synthesis and secretion and pancreatic Beta-cell dysfunction in diabetes. *Curr. Diabetes Rev.* 9, 25–53. [PubMed: 22974359]
- Fujimoto K, and Polonsky KS (2009). Pdx1 and other factors that regulate pancreatic beta-cell survival. *Diabetes Obes. Metab.* 11 (Suppl 4), 30–37. [PubMed: 19817786]
- Giddings SJ, Chirgwin J, and Permutt MA (1982). Effects of glucose on proinsulin messenger RNA in rats in vivo. *Diabetes* 31, 624–629. [PubMed: 6761201]
- González A, and Hall MN (2017). Nutrient sensing and TOR signaling in yeast and mammals. *EMBO J.* 36, 397–408. [PubMed: 28096180]
- Granot Z, Swisa A, Magenheimer J, Stolovich-Rain M, Fujimoto W, Manduchi E, Miki T, Lennerz JK, Stoeckert CJ Jr., Meyuhas O, et al. (2009). LKB1 regulates pancreatic beta cell size, polarity, and function. *Cell Metab.* 10, 296–308. [PubMed: 19808022]
- Hara K, Yonezawa K, Weng Q-P, Kozlowski MT, Belham C, and Avruch J (1998). Amino acid sufficiency and mTOR regulate p70 S6 kinase and eIF-4E BP1 through a common effector mechanism. *J. Biol. Chem* 273, 14484–14494. [PubMed: 9603962]
- Hara K, Maruki Y, Long X, Yoshino K, Oshiro N, Hidayat S, Tokunaga C, Avruch J, and Yonezawa K (2002). Raptor, a binding partner of target of rapamycin (TOR), mediates TOR action. *Cell* 110, 177–189. [PubMed: 12150926]
- Harmon JS, Stein R, and Robertson RP (2005). Oxidative stress-mediated, post-translational loss of MafA protein as a contributing mechanism to loss of insulin gene expression in glucotoxic beta cells. *J. Biol. Chem* 280, 11107–11113. [PubMed: 15664999]
- Helman A, Cangelosi AL, Davis JC, Pham Q, Rothman A, Faust AL, Straubhaar JR, Sabatini DM, and Melton DA (2020). A Nutrient-Sensing Transition at Birth Triggers Glucose-Responsive Insulin Secretion. *Cell Metab.* 31, 1004–1016.e5. [PubMed: 32375022]
- Henquin JC, and Rahier J (2011). Pancreatic alpha cell mass in European subjects with type 2 diabetes. *Diabetologia* 54, 1720–1725. [PubMed: 21465328]

- Horton JD, Goldstein JL, and Brown MS (2002). SREBPs: activators of the complete program of cholesterol and fatty acid synthesis in the liver. *J. Clin. Invest* 109, 1125–1131. [PubMed: 11994399]
- Hutagalung AH, and Novick PJ (2011). Role of Rab GTPases in membrane traffic and cell physiology. *Physiol. Rev* 91, 119–149. [PubMed: 21248164]
- Indra AK, Warot X, Brocard J, Bornert JM, Xiao JH, Chambon P, and Metzger D (1999). Temporally-controlled site-specific mutagenesis in the basal layer of the epidermis: comparison of the recombinase activity of the tamoxifen-inducible Cre-ER(T) and Cre-ER(T2) recombinases. *Nucleic Acids Res.* 27, 4324–4327. [PubMed: 10536138]
- Jewell JL, Russell RC, and Guan K-L (2013). Amino acid signalling upstream of mTOR. *Nat. Rev. Mol. Cell Biol.* 14, 133–139. [PubMed: 23361334]
- Jewell JL, Kim YC, Russell RC, Yu F-X, Park HW, Plouffe SW, Tagliabracci VS, and Guan K-L (2015). Metabolism. Differential regulation of mTORC1 by leucine and glutamine. *Science* 347, 194–198. [PubMed: 25567907]
- Jonas JC, Sharma A, Hasenkamp W, Ilkova H, Patané G, Laybutt R, Bonner-Weir S, and Weir GC (1999). Chronic hyperglycemia triggers loss of pancreatic beta cell differentiation in an animal model of diabetes. *J. Biol. Chem* 274, 14112–14121. [PubMed: 10318828]
- Kharroubi AT, and Darwish HM (2015). Diabetes mellitus: The epidemic of the century. *World J. Diabetes* 6, 850–867. [PubMed: 26131326]
- Kim DH, Sarbassov DD, Ali SM, King JE, Latek RR, Erdjument-Bromage H, Tempst P, and Sabatini DM (2002). mTOR interacts with raptor to form a nutrient-sensitive complex that signals to the cell growth machinery. *Cell* 110, 163–175. [PubMed: 12150925]
- Kim E, Goraksha-Hicks P, Li L, Neufeld TP, and Guan K-L (2008a). Regulation of TORC1 by Rag GTPases in nutrient response. *Nat. Cell Biol.* 10, 935–945. [PubMed: 18604198]
- Kim I, Xu W, and Reed JC (2008b). Cell death and endoplasmic reticulum stress: disease relevance and therapeutic opportunities. *Nat. Rev. Drug Discov.* 7, 1013–1030. [PubMed: 19043451]
- Lawlor N, George J, Bolisetty M, Kursawe R, Sun L, Sivakamasundari V, Kycia I, Robson P, and Stitzel ML (2017). Single-cell transcriptomes identify human islet cell signatures and reveal cell-type-specific expression changes in type 2 diabetes. *Genome Res.* 27, 208–222. [PubMed: 27864352]
- Leclerc GM, Boockfor FR, Faught WJ, and Frawley LS (2000). Development of a destabilized firefly luciferase enzyme for measurement of gene expression. *Biotechniques* 29, 590–591, 594–596, 598 passim. [PubMed: 10997273]
- Li X, Zhao X, Fang Y, Jiang X, Duong T, Fan C, Huang C-C, and Kain SR (1998). Generation of destabilized green fluorescent protein as a transcription reporter. *J. Biol. Chem* 273, 34970–34975. [PubMed: 9857028]
- Li H, Tsang CK, Watkins M, Bertram PG, and Zheng XF (2006). Nutrient regulates Tor1 nuclear localization and association with rDNA promoter. *Nature* 442, 1058–1061. [PubMed: 16900101]
- Liu X, Wang Z, Yang Y, Li Q, Zeng R, Kang J, and Wu J (2016). Rab1A mediates proinsulin to insulin conversion in β -cells by maintaining Golgi stability through interactions with golgin-84. *Protein Cell* 7, 692–696. [PubMed: 27502188]
- Loewith R, Jacinto E, Wullschlegel S, Lorberg A, Crespo JL, Bonenfant D, Oppliger W, Jenoe P, and Hall MN (2002). Two TOR complexes, only one of which is rapamycin sensitive, have distinct roles in cell growth control. *Mol. Cell* 10, 457–468. [PubMed: 12408816]
- Ma L, and Zheng J (2018). Single-cell gene expression analysis reveals β -cell dysfunction and deficit mechanisms in type 2 diabetes. *BMC Bioinformatics* 19 (Suppl 19), 515. [PubMed: 30598071]
- Macfarlane WM, McKinnon CM, Felton-Edkins ZA, Cragg H, James RF, and Docherty K (1999). Glucose stimulates translocation of the homeodomain transcription factor PDX1 from the cytoplasm to the nucleus in pancreatic beta-cells. *J. Biol. Chem.* 274, 1011–1016. [PubMed: 9873045]
- Martínez M, Martínez NA, and Silva WI (2017). Measurement of the Intracellular Calcium Concentration with Fura-2 AM Using a Fluorescence Plate Reader. *Bio-protocol* 7, e2411.
- Melloul D, Marshak S, and Cerasi E (2002). Regulation of insulin gene transcription. *Diabetologia* 45, 309–326. [PubMed: 11914736]

- Muoio DM, and Newgard CB (2008). Mechanisms of disease: Molecular and metabolic mechanisms of insulin resistance and β -cell failure in type 2 diabetes. *Nat. Rev. Mol. Cell Biol* 9, 193–205. [PubMed: 18200017]
- Newsholme P, Bender K, Kiely A, and Brennan L (2007). Amino acid metabolism, insulin secretion and diabetes. *Biochem. Soc. Trans* 35, 1180–1186. [PubMed: 17956307]
- Pahl HL (1999). Signal transduction from the endoplasmic reticulum to the cell nucleus. *Physiol. Rev* 79, 683–701. [PubMed: 10390516]
- Pallotta JA, and Kennedy PJ (1968). Response of plasma insulin and growth hormone to carbohydrate and protein feeding. *Metabolism* 17, 901–908. [PubMed: 4877988]
- Petersen HV, Peshavaria M, Pedersen AA, Philippe J, Stein R, Madsen OD, and Serup P (1998). Glucose stimulates the activation domain potential of the PDX-1 homeodomain transcription factor. *FEBS Lett.* 431, 362–366. [PubMed: 9714543]
- Plutner H, Cox AD, Pind S, Khosravi-Far R, Bourne JR, Schwaninger R, Der CJ, and Balch WE (1991). Rab1b regulates vesicular transport between the endoplasmic reticulum and successive Golgi compartments. *J. Cell Biol.* 115, 31–43. [PubMed: 1918138]
- Rabinowitz D, Merimee TJ, Maffezzoli R, and Burgess JA (1966). Patterns of hormonal release after glucose, protein, and glucose plus protein. *Lancet* 2, 454–456. [PubMed: 4161584]
- Rebsamen M, Pochini L, Stasyk T, de Araújo MEG, Galluccio M, Kandasamy RK, Snijder B, Fauster A, Rudashevskaya EL, Bruckner M, et al. (2015). SLC38A9 is a component of the lysosomal amino acid sensing machinery that controls mTORC1. *Nature* 519, 477–481. [PubMed: 25561175]
- Röder PV, Wu B, Liu Y, and Han W (2016). Pancreatic regulation of glucose homeostasis. *Exp. Mol. Med* 48, e219. [PubMed: 26964835]
- Ron D, and Walter P (2007). Signal integration in the endoplasmic reticulum unfolded protein response. *Nat. Rev. Mol. Cell Biol.* 8, 519–529. [PubMed: 17565364]
- Sancak Y, Peterson TR, Shaul YD, Lindquist RA, Thoreen CC, Bar-Peled L, and Sabatini DM (2008). The Rag GTPases bind raptor and mediate amino acid signaling to mTORC1. *Science* 320, 1496–1501. [PubMed: 18497260]
- Sancak Y, Bar-Peled L, Zoncu R, Markhard AL, Nada S, and Sabatini DM (2010). Ragulator-Rag complex targets mTORC1 to the lysosomal surface and is necessary for its activation by amino acids. *Cell* 141, 290–303. [PubMed: 20381137]
- Sanchez-Gurmaches J, and Guertin DA (2014). mTORC1 gRABs the Golgi. *Cancer Cell* 26, 601–603. [PubMed: 25517745]
- Saraste J, Lahtinen U, and Goud B (1995). Localization of the small GTP-binding protein rab1p to early compartments of the secretory pathway. *J. Cell Sci.* 108, 1541–1552. [PubMed: 7615674]
- Segerstolpe Å, Palasantza A, Eliasson P, Andersson E-M, Andréasson A-C, Sun X, Picelli S, Sabirsh A, Clausen M, Bjursell MK, et al. (2016). Single-Cell Transcriptome Profiling of Human Pancreatic Islets in Health and Type 2 Diabetes. *Cell Metab.* 24, 593–607. [PubMed: 27667667]
- Shimobayashi M, and Hall MN (2016). Multiple amino acid sensing inputs to mTORC1. *Cell Res.* 26, 7–20. [PubMed: 26658722]
- Soares MB, Schon E, Henderson A, Karathanasis SK, Cate R, Zeitlin S, Chirgwin J, and Efstratiadis A (1985). RNA-mediated gene duplication: the rat preproinsulin I gene is a functional retroposon. *Mol. Cell. Biol* 5, 2090–2103. [PubMed: 2427930]
- Stracka D, Jozefczuk S, Rudroff F, Sauer U, and Hall MN (2014). Nitrogen source activates TOR (target of rapamycin) complex 1 via glutamine and independently of Gtr/Rag proteins. *J. Biol. Chem* 289, 25010–25020. [PubMed: 25063813]
- Thomas JD, Zhang YJ, Wei YH, Cho JH, Morris LE, Wang HY, and Zheng XF (2014). Rab1A is an mTORC1 activator and a colorectal oncogene. *Cancer Cell* 26, 754–769. [PubMed: 25446900]
- Tsang CK, Chen M, Cheng X, Qi Y, Chen Y, Das I, Li X, Vallat B, Fu L-W, Qian C-N, et al. (2018). SOD1 Phosphorylation by mTORC1 Couples Nutrient Sensing and Redox Regulation. *Mol. Cell* 70, 502–515.e8. [PubMed: 29727620]
- Ventura A, Kirsch DG, McLaughlin ME, Tuveson DA, Grimm J, Lintault L, Newman J, Reczek EE, Weissleder R, and Jacks T (2007). Restoration of p53 function leads to tumour regression in vivo. *Nature* 445, 661–665. [PubMed: 17251932]

- Wang C-Y, and Liao JK (2012). A mouse model of diet-induced obesity and insulin resistance. *Methods Mol. Biol.* 821, 421–433. [PubMed: 22125082]
- Wang J, Davis S, Menon S, Zhang J, Ding J, Cervantes S, Miller E, Jiang Y, and Ferro-Novick S (2015). Ypt1/Rab1 regulates Hrr25/CK1δ kinase activity in ER-Golgi traffic and macroautophagy. *J. Cell Biol.* 210, 273–285. [PubMed: 26195667]
- Wei Y, Tsang CK, and Zheng XF (2009). Mechanisms of regulation of RNA polymerase III-dependent transcription by TORC1. *EMBO J.* 28, 2220–2230. [PubMed: 19574957]
- Wentworth BM, Schaefer IM, Villa-Komaroff L, and Chirgwin JM (1986). Characterization of the two nonallelic genes encoding mouse preproinsulin. *J. Mol. Evol.* 23, 305–312. [PubMed: 3104603]
- Wu G, Yussman MG, Barrett TJ, Hahn HS, Osinska H, Hilliard GM, Wang X, Toyokawa T, Yatani A, Lynch RA, et al. (2001). Increased myocardial Rab GTPase expression: a consequence and cause of cardiomyopathy. *Circ. Res.* 89, 1130–1137. [PubMed: 11739277]
- Wu T-J, Wang X, Zhang Y, Meng L, Kerrigan JE, Burley SK, and Zheng XF (2015). Identification of a Non-Gatekeeper Hot Spot for Drug-Resistant Mutations in mTOR Kinase. *Cell Rep.* 11, 446–459. [PubMed: 25865887]
- Xin Y, Kim J, Ni M, Wei Y, Okamoto H, Lee J, Adler C, Cavino K, Murphy AJ, Yancopoulos GD, et al. (2016a). Use of the Fluidigm C1 platform for RNA sequencing of single mouse pancreatic islet cells. *Proc. Natl. Acad. Sci. USA* 113, 3293–3298. [PubMed: 26951663]
- Xin Y, Kim J, Okamoto H, Ni M, Wei Y, Adler C, Murphy AJ, Yancopoulos GD, Lin C, and Gromada J (2016b). RNA Sequencing of Single Human Islet Cells Reveals Type 2 Diabetes Genes. *Cell Metab.* 24, 608–615. [PubMed: 27667665]
- Yang XZ, Li XX, Zhang YJ, Rodriguez-Rodriguez L, Xiang MQ, Wang HY, and Zheng XFS (2016). Rab1 in cell signaling, cancer and other diseases. *Oncogene* 35, 5699–5704. [PubMed: 27041585]
- Zhang Y, Wang X, Qin X, Wang X, Liu F, White E, and Zheng XFS (2015). PP2AC Level Determines Differential Programming of p38-TSC-mTOR Signaling and Therapeutic Response to p38-Targeted Therapy in Colorectal Cancer. *EBioMedicine* 2, 1944–1956. [PubMed: 26844273]
- Zhang H, Li XX, Yang Y, Zhang Y, Wang HY, and Zheng XFS (2018). Significance and mechanism of androgen receptor overexpression and androgen receptor/mechanistic target of rapamycin cross-talk in hepatocellular carcinoma. *Hepatology* 67, 2271–2286. [PubMed: 29220539]
- Zhang Q, Pan Y, Zeng B, Zheng X, Wang H, Shen X, Li H, Jiang Q, Zhao J, Meng Z-X, et al. (2019). Intestinal lysozyme liberates Nod1 ligands from microbes to direct insulin trafficking in pancreatic beta cells. *Cell Res.* 29, 516–532. [PubMed: 31201384]
- Zoncu R, Bar-Peled L, Efeyan A, Wang S, Sancak Y, and Sabatini DM (2011). mTORC1 senses lysosomal amino acids through an inside-out mechanism that requires the vacuolar H(+)-ATPase. *Science* 334, 678–683. [PubMed: 22053050]

Highlights

- Rab1A regulates mTORC1 signaling in response to amino acids (aas) in beta-cells
- Rab1A knockout mice are deficient of insulin expression and hyperglycemic
- Branched chain aas regulate insulin transcription through mTORC1-Rab1A-PDX1 axis
- Amino acids regulate beta-cell trans-differentiation through mTORC1-Rab1A-PDX1 axis

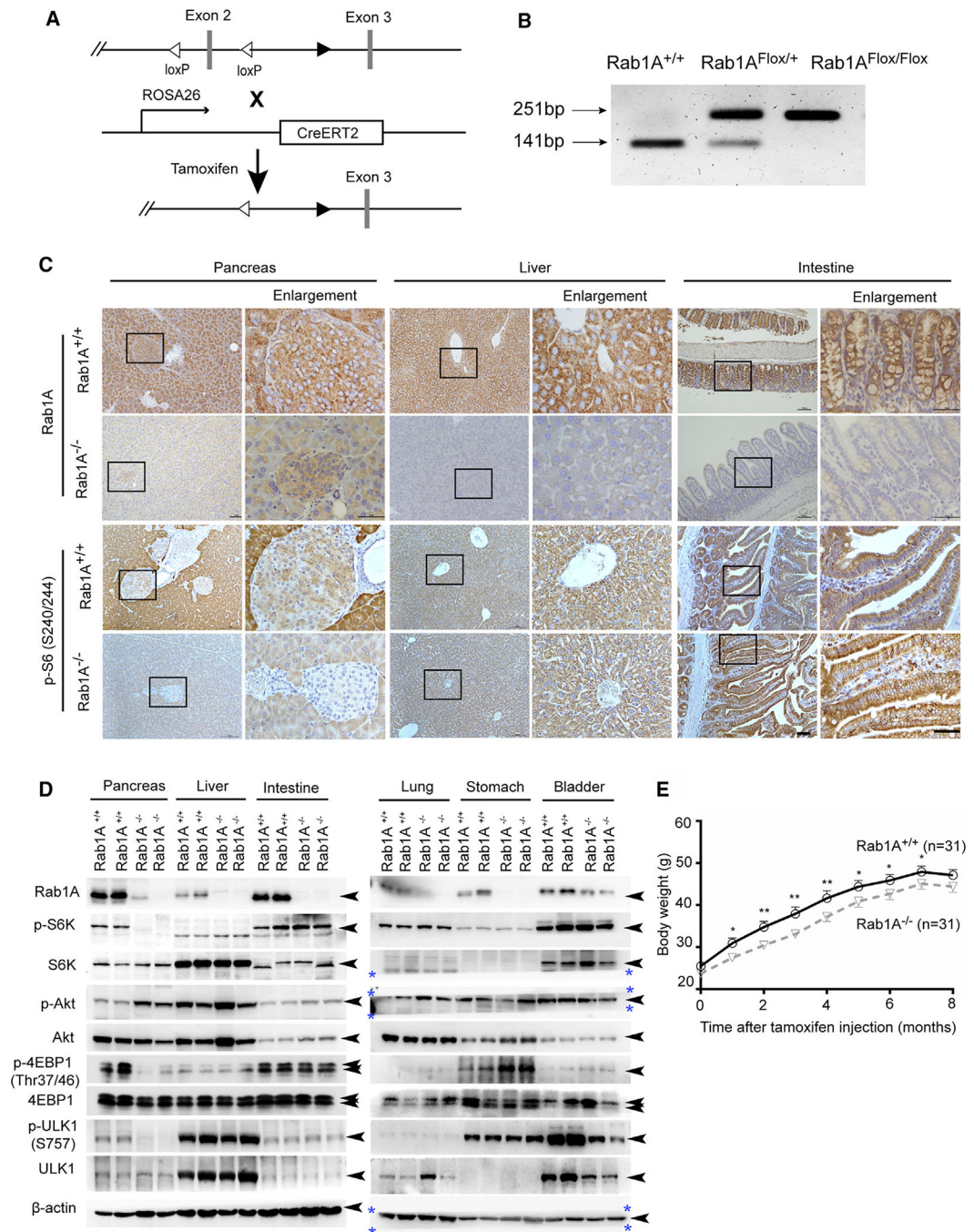


Figure 1. Inducible Rab1A knockout in adult mice leads to inhibition of pancreatic mTORC1 signaling, hyperglycemia and glucose intolerance

(A) Design of TAM-inducible Rab1A knockout in adult mice.

(B) TAM was administered to R26-Cre-ERT2^{+/-}; Rab1A^{Flox/Flox} and Rab1A^{Flox/Flox} mice at 6 weeks of age. Analysis of RAB1A protein expression by immunoblot in different tissues in Rab1A^{+/+} and Rab1A^{-/-} mice 1 week post TAM.

(C) Rab1A knockout selectively inhibits mTORC1 signaling in pancreatic islets. Rab1A protein expression and mTORC1 signaling (p-S6) were examined by immunohistochemistry

(IHC) analysis of the pancreas, liver, and intestine tissues in Rab1A^{+/+} and Rab1A^{-/-} mice (1 week post TAM). Shown are representative IHC images. Scale bars, 50 μ m and 100 μ m. (D) Rab1A knockout selectively inhibits mTORC1 signaling in pancreatic islets. Rab1A knockout and the effect on mTORC1 signaling were examined by immunoblot of Rab1A and phosphorylation of mTORC1 substrates (S6K, 4EBP1, and Ulk1) in the pancreas, liver, intestine, lung, stomach, and bladder tissues in Rab1A^{+/+} and Rab1A^{-/-} mice (1 week post TAM). Arrows show bands representing different proteins. Asterisk marks the borders of the original immunoblot.

(E) TAM was administered to R26-Cre-ERT2^{+/-}; Rab1A^{Flox/Flox} and Rab1A^{Flox/Flox} mice at 6 weeks of age. Weight changes of Rab1A^{+/+} (n = 31) and Rab1A^{-/-} (n = 31) mice was monitored monthly. Results are presented as mean \pm SEM (n = 31). *p < 0.05, **p < 0.01, unpaired Student's t test.

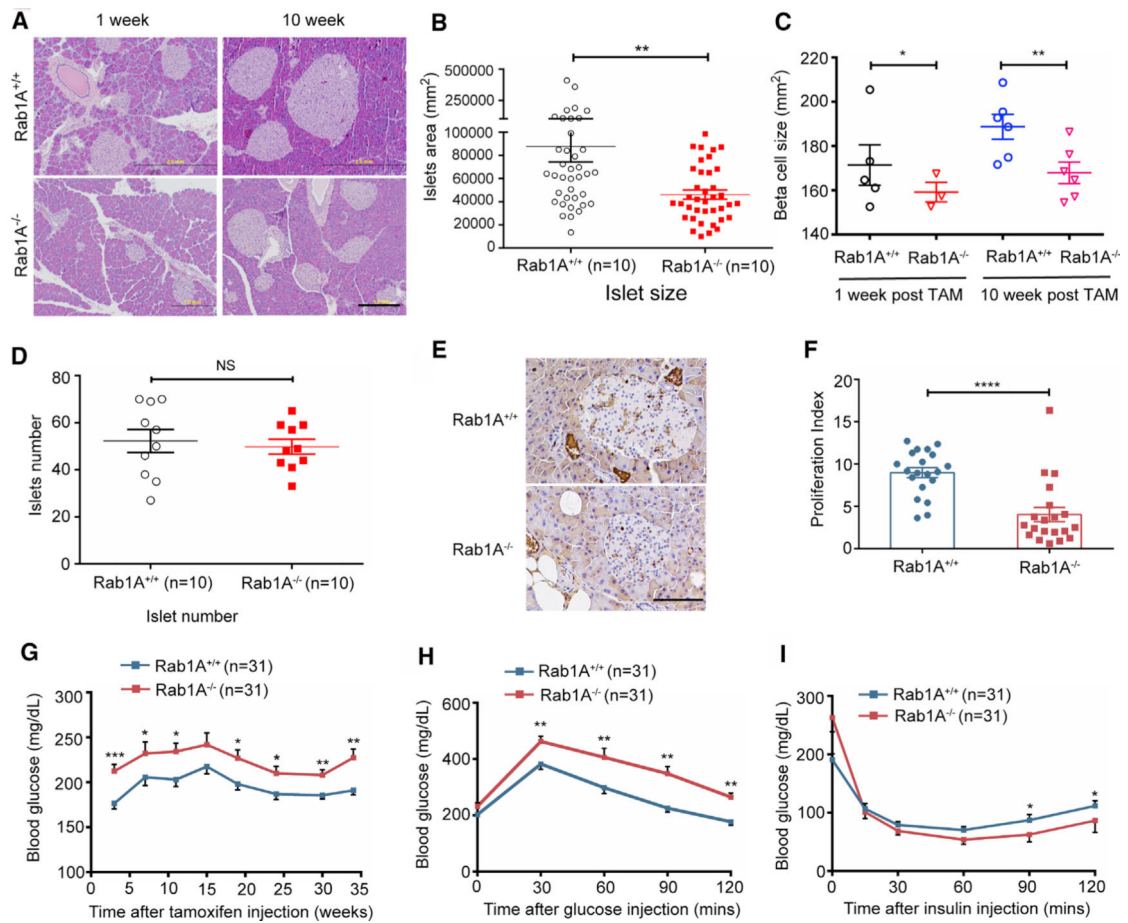


Figure 2. Rab1A is required for proliferation of pancreatic islet cells

(A) Rab1A ablation markedly decreases pancreatic islet size in mice as shown by hematoxylin and eosin (H&E) staining of pancreatic sections (1 and 10 weeks post TAM). Lighted stained areas are islets. Scale bars, 1 mm.

(B) Islet areas were quantified using ImageJ software. Rab1A^{+/+} (n = 10) and Rab1A^{-/-} mice (n = 10). **p < 0.01, unpaired Student's t test.

(C) Rab1A knockout leads to a decrease in β -cell size. β -cell size was measured in Rab1A^{-/-} mice (n = 3) and Rab1A^{+/+} mice (n = 3). *p < 0.05, **p < 0.01, unpaired Student's t test.

(D) Rab1A knockout does not affect total number of islets. Same as c except the number of islets were counted. Rab1A^{+/+} (n = 10) and Rab1A^{-/-} mice (n = 10). NS, not significant. Paired Student's t test was performed.

(E) Rab1A knockout inhibits islet cell proliferation. Shown is Ki-67 stained pancreatic tissue sections. Dotted area indicates islets. Scale bars, 100 μ m.

(F) Proliferation index as calculated by the percentage of Ki-67⁺ cells per islet in Rab1A^{+/+} (n = 10) and Rab1A^{-/-} pancreases (n = 10). Animals from 10 weeks post TAM unless otherwise noted.

(G) Rab1A knockout leads to hyperglycemia. 6 h fasting blood glucose level was monitored monthly in Rab1A^{+/+} (n = 31) and Rab1A^{-/-} mice (n = 31).

(H) Rab1A knockout leads to glucose intolerance. Intraperitoneal glucose tolerance tests were performed in Rab1A^{+/+} (n = 31) and Rab1A^{-/-} mice (n = 31) at 3 weeks post TAM. Blood glucose levels were measured every 30 min after glucose injection.

(I) Insulin sensitivity remains normal in Rab1A knockout animals. Intraperitoneal insulin tolerance tests were performed in Rab1A^{+/+} (n = 31) and Rab1A^{-/-} (n = 31) mice (6 weeks post TAM).

All results are presented as mean \pm SEM. *p < 0.05, **p < 0.01, ***p < 0.001, ****p < 0.0001, unpaired Student's t test for two groups unless otherwise indicated.

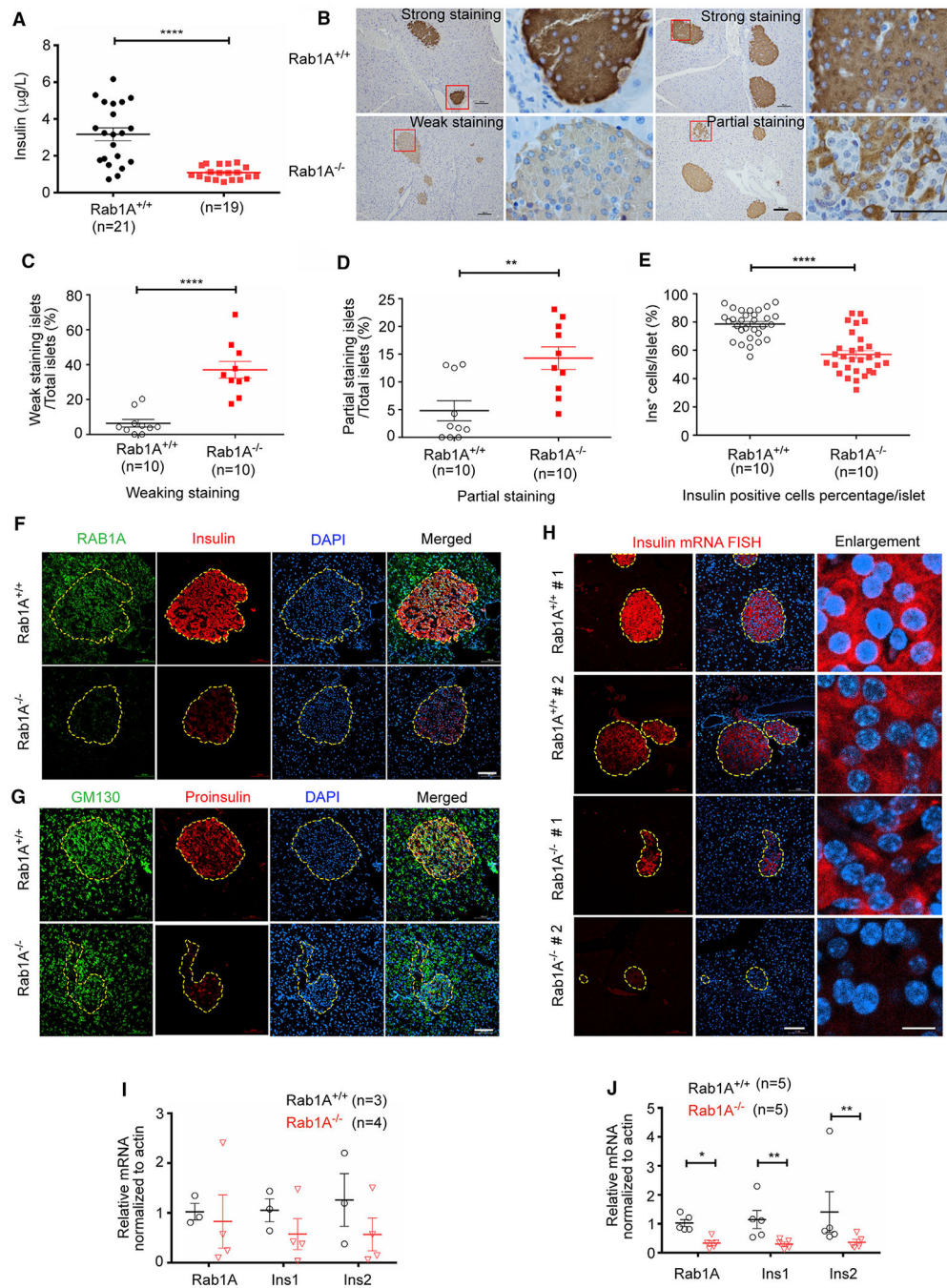


Figure 3. Rab1A is required for insulin expression in adult mice

(A) Rab1A knockout leads to reduced blood insulin level. Blood insulin was measured by ELISA at 15 mins after administration of glucose by IP in Rab1A^{+/+} (n = 21) and Rab1A^{-/-} (n = 19) mice.

(B–E) Rab1A knockout leads to reduced insulin protein expression in pancreatic islets as judged by IHC. IHC staining of insulin protein in pancreatic tissues from Rab1A^{+/+} and Rab1A^{-/-} mice. Shown are representative images of strong, weak and partial insulin staining. “Strong” refers to intense staining as seen in WT; “weak” refers to unformed

reduction in insulin expression; “partial” refers to a mosaic phenotype in which patches of islets have lost insulin expression. Scale bars, 50 μm and 100 μm . Percentage of islets with weak (C) and partial (D) insulin staining in Rab1A^{+/+} (n = 10) and Rab1A^{-/-} (n = 10) mice. Boxed areas were enlarged to show details. Rab1A knockout leads to reduced blood insulin level. Percentage of insulin⁺ cells in islets with partial insulin staining (E) in Rab1A^{+/+} (n = 10) and Rab1A^{-/-} (n = 10) mice.

(F) Rab1A knockout leads to reduced insulin protein expression in pancreatic islets as judged by IF. IF analysis of Rab1A (green) and Insulin protein (red) in Rab1A^{+/+} and Rab1A^{-/-} pancreatic tissue sections. Scale bars, 100 μm . Dotted areas are pancreatic islets.

(G) Rab1A knockout leads to reduced proinsulin protein expression in pancreatic islets as judged by IF. IF analysis of GM130 (green) and proinsulin protein (red) in Rab1A^{+/+} and Rab1A^{-/-} pancreatic tissue sections. Scale bars, 100 μm .

(H) Rab1A knockout leads to reduced insulin mRNA expression in pancreatic islets. FISH analysis of insulin mRNA (red) and Rab1A (green) in Rab1A^{+/+} and Rab1A^{-/-} pancreatic tissue sections. Scale bars, 100 μm and 10 μm . Shown are staining of pancreas from two different animals in each group.

(I and J) Real-time PCR analysis of Rab1A, Ins1, and Ins2 mRNA in Rab1A^{+/+} and Rab1A^{-/-} pancreas at 3.5 (I) and 18 (J) weeks post TAM. n = 3 from each group in (I) and n = 5 from each group in (J).

All results are presented as mean \pm SEM. *p < 0.05, **p < 0.01, ***p < 0.001, ****p < 0.0001, unpaired Student's t test for two groups unless otherwise indicated.

Animals from 10 weeks post TAM unless otherwise noted.

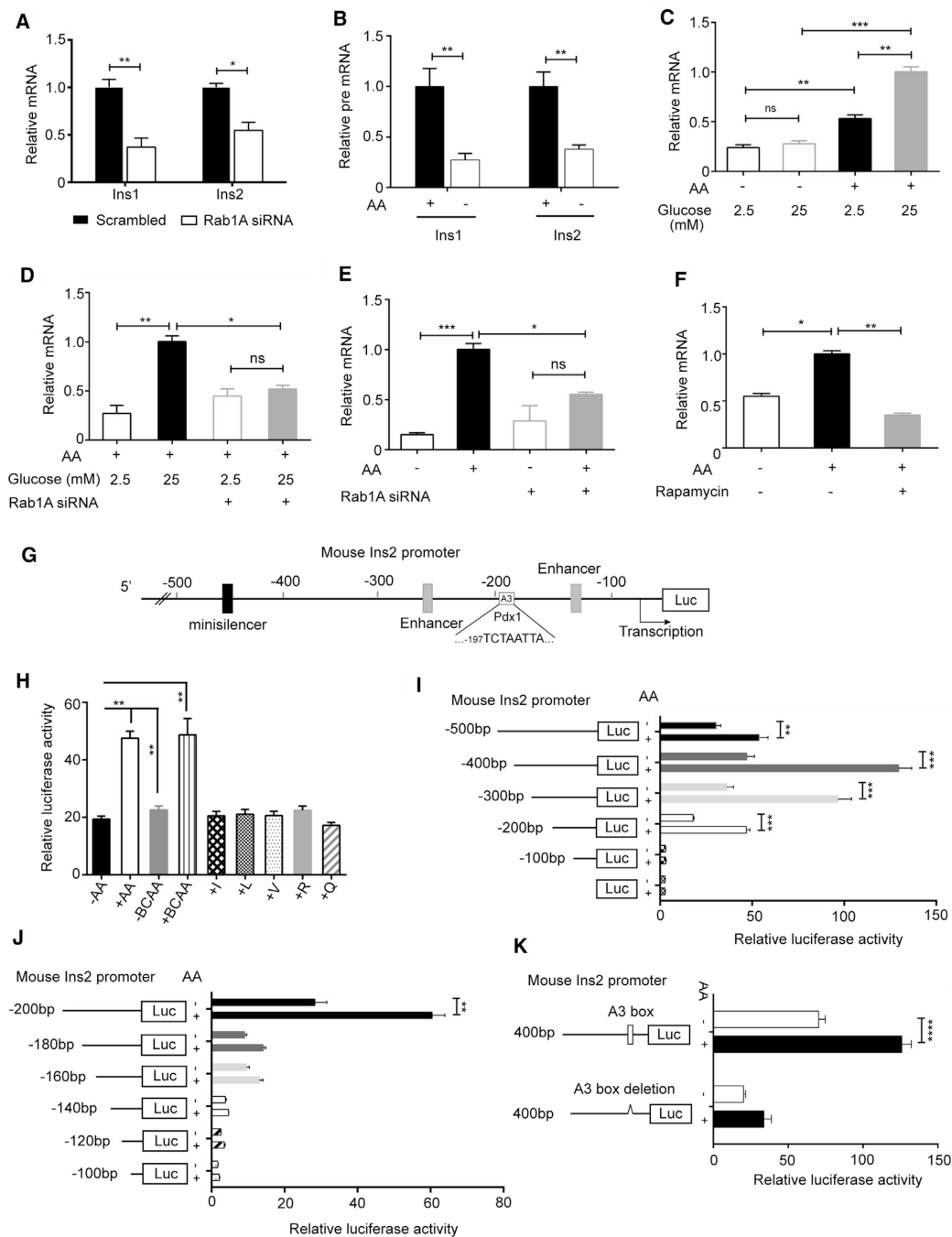


Figure 4. Amino acids activate insulin transcription in a Rab1A- and mTORC1-dependent manner

(A) Rab1A is required for insulin mRNA expression. MIN6 cells in complete medium were treated with Rab1A or control siRNAs for 24 h. Ins1 and Ins2 mRNA was measured by qRT-PCR. Four replicates were used (n = 4).

(B) Amino acid starvation inhibits insulin mRNA expression. MIN6 cells were cultured in normal or aa starvation medium for 2 h. Ins1 and Ins2 mRNA expression was determined by qRT-PCR. Triplicates were used (n = 3).

(C) Amino acid is required for glucose to stimulate insulin mRNA expression. MIN6 cells were cultured in low (2.5 mM) or high (25 mM) glucose in the presence or absence of aa for 2 h. Ins2 mRNA expression was determined by qRT-PCR. Triplicates were used (n = 3).

(D) Rab1A is required for glucose to stimulate insulin mRNA expression. MIN6 cells transfected with Rab1A or control siRNA for 24 h and then cultured in 5 mM or 25 mM glucose for 2 h. Ins2 mRNA was determined by qRT-PCR. Triplicates were used (n = 3).

(E) Rab1A is required for aas to stimulate insulin mRNA expression. MIN6 cells transfected with Rab1A or control siRNA were starved from aa for 24 h and then stimulated with aas for 2 h. Ins2 mRNA was determined by qRT-PCR. Triplicates were used (n = 3).

(F) mTORC1 is required for aas to stimulate insulin mRNA expression. Starved MIN6 cells were stimulated with aas in 25 mM glucose for 2 h in the absence or presence of 100 nM rapamycin. Ins2 mRNA was determined by qRT-PCR. Triplicates were used (n = 3).

(G) Construct of Ins2 promoter-luciferase reporter. The structure organization of a 500 bp mouse Ins2 promoter is shown. Boxes are motifs important for Ins2 promoter activity in response to aas.

(H) Branched chain amino acids (BCAA) together activate insulin transcription. MIN6 cells carrying a Luc-PEST (Luc) reporter under the control of Ins2 promoter was starved from aas and restimulated with full aas, BCAA, leucine, isoleucine, valine, glutamine, or arginine for 2 h and measured for Luc activity. Four replicates were used (n = 4).

(I) Deletional analysis of the 500 bp mouse Ins2 promoter region by 100-bp increments using the Luc-PEST reporter assay in MIN6 cells starved from aas and restimulated for 2 h. Four replicates were used (n = 4).

(J) Deletional analysis of the 200 bp mouse Ins2 promoter region by 20-bp increments using the Luc-PEST reporter assay in MIN6 cells. Five replicates were used (n = 5).

(K) A3 box is required for aas to stimulate Ins2 promoter. Effect of A3 box deletion in the 400 bp region of mouse Ins2 promoter. Triplicates were used (n = 3).

All results were presented as mean \pm SEM of three independent experiments indicated as above. Representative results were shown. *p < 0.05, **p < 0.01, ***p < 0.001, ****p < 0.0001. Unpaired Student's t test for two groups.

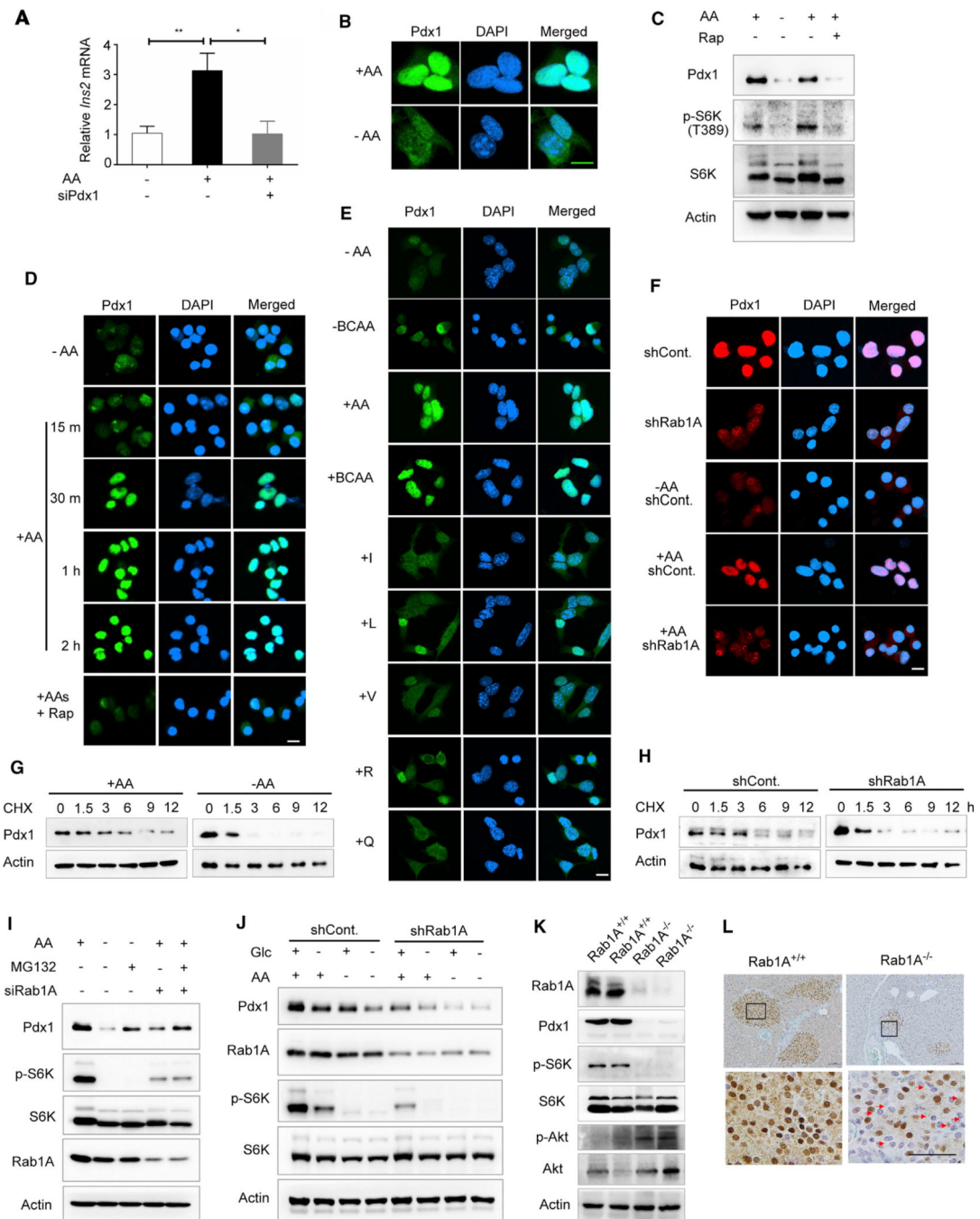


Figure 5. Amino acids promotes the stability and nuclear localization of Pdx1 in a Rab1A- and mTORC1-dependent manner

(A) Pdx1 is required for aas to stimulate insulin mRNA expression. MIN6 cells transfected with Pdx1 or control siRNA were starved for 24 h and stimulated with aas for 2 h. *Ins2* mRNA expression was assayed by qRT-PCR. Results are presented as mean \pm SEM of three independent experiments (n = 3). *p < 0.05, **p < 0.01, unpaired Student's t test for two groups.

- (B) Amino acids are required for maintaining Pdx1 protein level and nuclear localization. MIN6 cells were cultured in normal or aa starvation medium for 24 h. Pdx1 protein (green) was analyzed by IF staining. Scale bars, 10 μ m.
- (C) Amino acids promote Pdx1 protein level in an mTORC1-dependent manner. MIN6 cells were starved from aas for 24 h and re-stimulated for 2 h in the absence or presence of 100 nM rapamycin. Samples were analyzed by immunoblot.
- (D) Amino acids promote Pdx1 protein level and nuclear localization in an mTORC1-dependent manner. MIN6 cells were starved from aas for 24 h and were then re-stimulated with aas for different times in the absence or presence of 100 nM rapamycin. Pdx1 (green) was analyzed by IF staining. Scale bars, 10 μ m.
- (E) Branched chain amino acids (BCAA) promote Pdx1 nuclear accumulation. MIN6 cells was starved from full aas and restimulated with full aas, BCAA, leucine, isoleucine, valine, glutamine or arginine for 2 h, and Pdx1 was analyzed by immunofluorescence staining. Scale bars, 10 μ m.
- (F) Amino acids promote Pdx1 protein level and nuclear localization in n Rab1A-dependent manner. MIN6 cells were transfected with control or Rab1A short hairpin RNA (shRNA) and starved of aas for 24 h before re-stimulated with aas for 2 h. Pdx1 was analyzed by IF. Scale bars, 10 μ m.
- (G) Amino acids regulate Pdx1 protein stability. MIN6 cells were cultured in normal medium (+aa) or aa starvation medium (-aa) for 24 h and then treated with cycloheximide (CHX) for different times. PDX1 protein was analyzed by immunoblot. Actin was used as a loading control.
- (H) Rab1A is required for maintaining Pdx1 protein stability. MIN6 cells were transfected with control or Rab1A shRNA, and then treated with CHX for different times. Pdx1 protein was analyzed by immunoblot.
- (I) aa-Rab1A signaling regulates proteasome-dependent degradation of Pdx1. MIN6 cells starved from aas and then re-stimulated with aas without or with Rab1A knockdown in the absence or presence of MG-132. Pdx1 protein was analyzed by immunoblot.
- (J) Amino acids and glucose cooperate in the regulation of Pdx1 stability. MIN6 cells starved from aas and glucose and then re-stimulated with aas and/or glucose without or with Rab1A knockdown. Pdx1 protein was analyzed by immunoblot.
- (K) Rab1A knockout leads to downregulation of Pdx1 protein expression and mTORC1 signaling. Pdx1, p-S6K, S6K, p-Akt, and Akt were analyzed by immunoblot analysis of the pancreas of Rab1A^{+/+} and Rab1A^{-/-} mice (1 week post TAM). Shown are two different animals in each group.
- (L) Same as (K) except Pdx1 was analyzed by IHC. Arrowheads indicate loss of Pdx1 in the nucleus. Scale bar, 50 μ m.

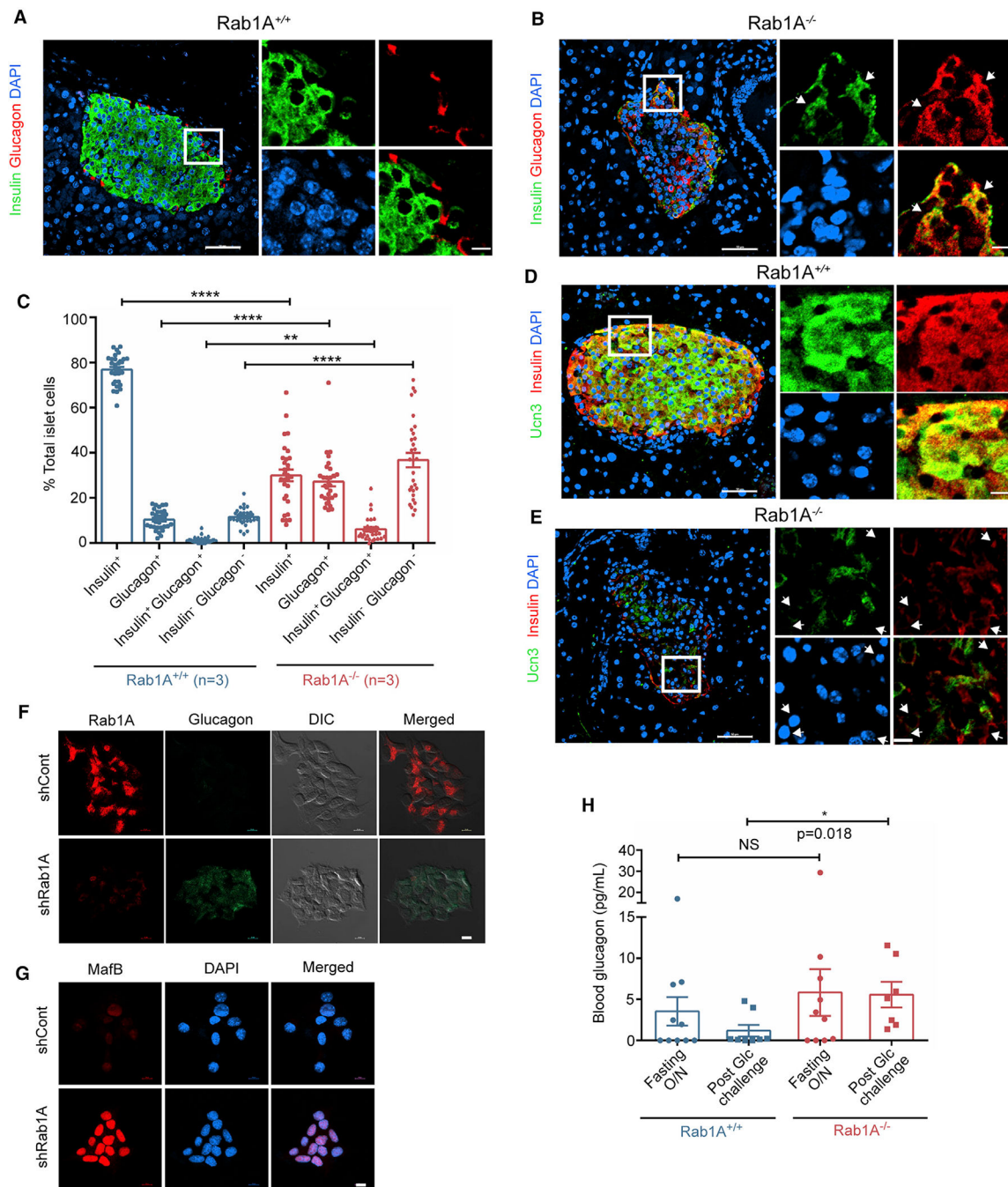


Figure 6. Rab1A maintains mature β -cells and regulates *trans*-differentiation of β -cells to α -cells (A–C) Rab1A knockout leads to loss of β -cells and gain of α -cells in mice. Co-staining of insulin (green) and glucagon (red) by IF in Rab1A^{+/+} (A) and Rab1A^{-/-} (B) pancreas (2 weeks post TAM). Arrowheads show insulin⁺glucagon⁺ cells. Boxed areas are enlarged to show details. Arrowheads indicate. Scale bars, 50 μ m and 10 μ m. (C) Quantification of different cell populations in (A) and (B). n = 3 mice from each group, where 10 islets from each mouse were evaluated. Results were presented as mean \pm SEM. **p < 0.01, ****p < 0.0001. Unpaired Student's t test for two groups.

(D-E) Rab1A knockout causes loss of mature β -cells. Co-staining of Ucn3 (green) and insulin (red) in Rab1A^{+/+} (D) and Rab1A^{-/-} (E) pancreas (2 week post TAM). Boxed areas were enlarged to show details. Arrowheads indicate Ucn3⁻ insulin⁺. Scale bars, 50 μ m and 10 μ m.

(F) Rab1A knockdown in β -cells results in glucagon expression. MIN6 cells were transfected with control or Rab1A shRNA. Rab1A (red) and glucagon (green) proteins were analyzed by IF staining. Scale bar, 10 μ m.

(G) Rab1A knockdown drives *trans*-differentiation from β -cells to α -cells. MIN6 cells were transfected with control or Rab1A shRNA. MafB protein was analyzed by IF staining. Scale bar, 10 μ m.

(H) Rab1A knockout causes deregulation of blood glucagon. Blood glucagon level was determined by ELISA after overnight fasting and glucose re-stimulation in Rab1A^{+/+} and Rab1A^{-/-} mice (2 weeks post TAM). Unpaired Student's t test, * $p < 0.05$. Results were presented as mean \pm SEM. $n = 10, 8, 10,$ and 7 for controlfasting, control-post glucose challenge, Rab1A^{-/-}-fasting, and Rab1A^{-/-}-post glucose challenge groups, respectively.

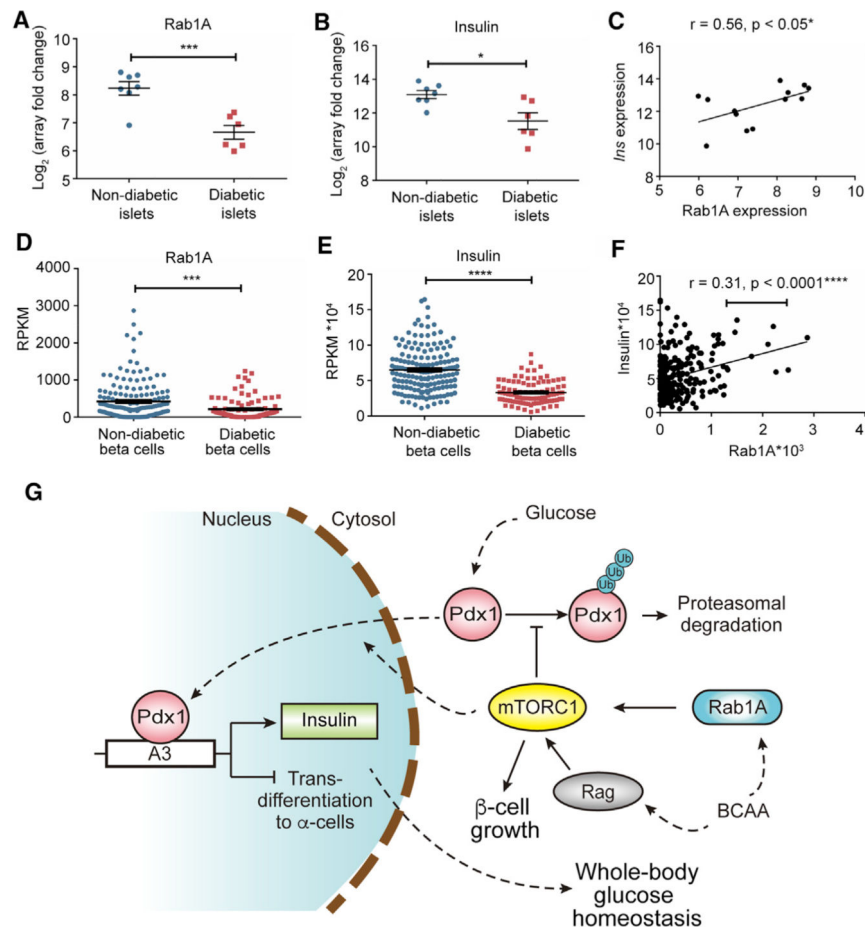


Figure 7. Downregulation of Rab1A in β -cells in T2DM, which is correlated with reduced insulin expression and elevated glucagon expression

(A and B) Downregulation of both Rab1A and insulin mRNA expression in healthy and T2DM islets (GEO: GSE25724). Non-diabetic islets, $n = 7$; diabetic islets, $n = 6$.

(C) Correlation in the downregulation of Rab1A and insulin mRNA expression. Correlation of Rab1A and insulin expression was analyzed using Pearson analysis in the GEO dataset (GSE25724).

(D and E) Downregulation of both Rab1A and insulin mRNA in individual healthy and T2DM β -cells. Analysis of Rab1A and insulin mRNA expression in the scRNA-seq dataset GSE86469. Non-diabetic beta cells, $n = 168$; Diabetic beta cells, $n = 96$.

(F) Downregulation of Rab1A and insulin mRNA expression in individual β -cells.

Correlation of Rab1A and insulin expression was analyzed using Pearson analysis in GSE86469.

(G) A working model for aa/BCAA-mTORC1 signaling to regulate insulin transcription, β -cell growth, and *trans*-differentiation in the control of whole-body glucose homeostasis.

All results were presented as mean \pm SEM. * $p < 0.05$, *** $p < 0.001$, **** $p < 0.0001$.

Unpaired Student's t test for two groups.

KEY RESOURCES TABLE

REAGENT or RESOURCE	SOURCE	IDENTIFIER
Antibodies		
Rabbit polyclonal anti-Rab1A	Proteintech	Cat#11671-1-AP; RRID: AB_2173437
Goat polyclonal anti-Rab1A	Abcam	Cat# ab211524; RRID: AB_2313773
Rabbit monoclonal anti-p70 S6K	Cell Signaling Technology	Cat# 2708; RRID: AB_390722
Rabbit monoclonal anti-phospho-p70 S6K (Thr389)	Cell Signaling Technology	Cat# 9234; RRID: AB_2269803
Rabbit monoclonal anti-phospho-Akt (Ser473)	Cell Signaling Technology	Cat# 4060; RRID: AB_2313773
Mouse monoclonal anti-Akt (Pan)	Cell Signaling Technology	Cat# 2920; RRID: AB_1147620
Rabbit monoclonal anti- β -Actin	Cell Signaling Technology	Cat# 8457; RRID: AB_10950489
Mouse monoclonal anti-Ki-67 Clone B56	BD PharMingen	Cat# 550609; RRID: AB_393778
Rabbit monoclonal anti-Insulin	Abcam	Cat# ab181547; RRID: AB_2716761
Mouse monoclonal anti-Insulin Clone No.:4B6A7	Proteintech	Cat# 66198-1-Ig; RRID: AB_2313773
Rabbit polyclonal anti-GM130/GOLGA2	Novus biologicals	Cat# NBP2-53420; RRID: AB_2313773
Mouse monoclonal anti-Proinsulin (253627)	Novus biologicals	Cat# MAB13361; RRID: AB_2126534
Rabbit monoclonal anti-Pdx1	Cell Signaling Technology	Cat# 5679; RRID: AB_10706174
Rabbit monoclonal anti-Pdx1	Abcam	Cat# ab219207; RRID: AB_2313773
Rabbit monoclonal anti-Glucagon (EP3070)	Abcam	Cat# ab92517; RRID: AB_10561971
Mouse monoclonal anti-Glucagon (K79bB10)	Abcam	Cat# ab10988; RRID: AB_297642
Rabbit monoclonal anti-MafB (BLR046F)	Bethyl laboratories	Cat# A700-046; RRID: AB_2313773
Rabbit polyclonal anti-Urocortin III IgG	Phoenix Pharmaceuticals	Cat# G-019-29 Lot: 00741; RRID: AB_2313773
Rabbit monoclonal anti-phospho-4E-BP1 (Thr37/46)	Cell Signaling Technology	Cat# 2855; RRID: AB_2313773
Rabbit monoclonal anti-4E-BP1 (53H11)	Cell Signaling Technology	Cat# 9644; RRID: AB_2097841
Rabbit monoclonal anti-phospho-ULK1 (Ser757)	Cell Signaling Technology	Cat# 6888; RRID: AB_10829226
Rabbit monoclonal anti-ULK1 (D8H5)	Cell Signaling Technology	Cat# 8054; RRID: AB_11178668
Rabbit monoclonal anti-phospho-S6 Ribosomal Protein (Ser240/244) (D68F8)	Cell Signaling Technology	Cat# 5364; RRID: AB_10694233
Mouse monoclonal ANTI-FLAG® M2 antibody	Sigma Aldrich	Cat# F3165; RRID: AB_259529
Biological samples		
Mouse whole blood	This paper	N/A
Mouse serum	This paper	N/A
Chemicals, peptides, and recombinant proteins		
Rapamycin	LC Laboratories	#53123-88-9
Cycloheximide	Sigma Aldrich	#C7698
MG-132	Sigma Aldrich	#M7449
Tamoxifen	Sigma Aldrich	# T5648
D-(+)-Glucose	Sigma Aldrich	#G7021
Human Insulin solution	Novo Nordisk	#0169-1833-11
Actinomycin D	Sigma Aldrich	# A9415

REAGENT or RESOURCE	SOURCE	IDENTIFIER
(Z)-4-Hydroxytamoxifen	Sigma Aldrich	#H7904
Critical commercial assays		
Mouse Insulin ELISA Kit	Mercodia	#10-1247-01; RRID: AB_2783837
Rodent Glucagon ELISA Kit	Mercodia	#10-1281-01; RRID: AB_2783839
Rat/Mouse Proinsulin ELISA kit	Mercodia	#10-1232-01
Blood glucose meter and test strips	Alliance International	#I-QARE DS-A
Stellaris® FISH Probes, Mouse Ins1/2 with Quasar® 570 Dye	LGC Biosearch tech	#VSMF-3611-5
Fluo-4 Direct Calcium Assay Kit	Thermo fisher	# F10471
Guanosine 5-triphosphate-Agarose	Sigma Aldrich	G9768
Deposited data		
GSE25724	Dominguez et al., 2011	N/A
GSE86469	Lawlor et al., 2017	N/A
GSE81608	Xin et al., 2016b	N/A
Experimental models: cell lines		
MIN6	Dr. Radovick lab	RRID: CVCL_0431
INS-1 823/13	Dr. Radovick lab	RRID: CVCL_7226
293T	ATCC	#CRL-3216
Experimental models: organisms/strains		
Mouse Rab1A ^{flox/flox} , C57BL6	This paper	N/A
B6.129-Gt(ROSA)26Sor ^{tm1(cre/ERT2)Tyj/J}	Jackson Laboratories	#008463; RRID: IMSR_JAX:008463
Oligonucleotides		
Primer for deleting A3 box of Ins2 promoter forward primer, GTTAAGACCCCTAGGACTAAGTAGAG	This paper	N/A
Primer for deleting A3 box of Ins2 promoter reverse primer, GTCCTAGGGTCTTAACAAGG	This paper	N/A
Mouse Pdx1 siRNA #1, GGGAACUUAACCUAGGCGUTT	Babu et al., 2008	N/A
Mouse Pdx1 siRNA #2	Babu et al., 2008	N/A
Mouse Pdx1 siRNA #3 Sigma esiRNA	Sigma Aldrich	#EMU046321
Mouse shRab1A #1: GGTGGAAAGTCCTGCCTTCT	This paper	N/A
Mouse shRab1A #2: GCACAATTGGTGTGGATTCA	This paper	N/A
Mouse shRab1A #3: GGAGTCCTTCAATAACGTAA	This paper	N/A
Mouse shRab1A #4: GCAACGAATGTAGAACAGTCT	This paper	N/A
Real time PCR primers		
Pdx1-F: CCCAGTTTACAAGCTCGCT	This paper	N/A
Pdx1-R: CTCGGTCCATTCGGGAAAGG	This paper	N/A
Rab1A-F: CAGTGCTAAGAACGCAACGA	This paper	N/A
Rab1A-R: CTTGACTGGAGTGCTCTGGA	This paper	N/A

REAGENT or RESOURCE	SOURCE	IDENTIFIER
RatINS-1-F: CGCTTCCTGCCCTGCTGGC	This paper	N/A
RatINS-1-R: GGACCACAAAGGTGCTGTTTGA	This paper	N/A
RatINS-2-F: TTTGTGGTTCTCACTTGGTG	This paper	N/A
RatINS-2-R: ATCCACGATGCCGCGCTTCTG	This paper	N/A
RtIns1-pre-F: GTTCTCTCTTACATGG	This paper	N/A
RtIns1-pre-R: GGCTCCCAGAGGACGA	This paper	N/A
RtIns2-pre-F: TTCTACACACCCATGTCC	This paper	N/A
RtIns2-pre-R: CACAATTTACAAGGTCTC	This paper	N/A
RtIns2 mature-F: TGGATCCGCTTCCTGC	This paper	N/A
RtIns2 mature-R: TAGAGAGCTTCCACC	This paper	N/A
MsIns1 pre-F: GGATCTTTGCTAGCCT	This paper	N/A
MsIns1 pre-R: GACAAAAGCCTGGGTGG	This paper	N/A
MsIns2 pre-F: TGTGGGGAGCGTGGCTT	This paper	N/A
MsIns2 pre-R: CAAGTGTGAAGAAAACC	This paper	N/A
MsIns2 mature-F: TGCCCTGCTGGCCCT	This paper	N/A
MsIns2 mature-R: CACCAGGTAGAGAGCCT	This paper	N/A
RatActin-F: GGCCGTCTTCCCCTCCATCG	This paper	N/A
RatActin-R: CCAGTTGGTGACAATGCCGTGT	This paper	N/A
Mouse-Actb-F: CTAGTAACCGAGACAT	This paper	N/A
Mouse-Actb-R: GGACGCCACAGCGGCC	This paper	N/A
Recombinant DNA		
pGLV-H1-GFP&Puro	Genepharma	N/A
pRSV-Rev	Addgene	#12253; RRID: Addgene_12253
pMDLg/pRRE	Addgene	#12251; RRID: Addgene_12251
pCMV-VSV-G	Addgene	#8454; RRID: Addgene_8454
Myc-DDK-tagged Rab1A	ORIGENE	CAT#: MR202153
Mouse RagA shRNA #1	Sigma Aldrich	TRCN0000337548
Mouse RagA shRNA #2	Sigma Aldrich	TRCN0000311262
Mouse RagB shRNA #1	Sigma Aldrich	TRCN0000102658
Mouse RagB shRNA #2	Sigma Aldrich	TRCN0000102656
pGL4.84	Promega	#E752A
pGL4.84-Ins2 promoter-up-100bps	This paper	N/A
pGL4.84-Ins2 promoter -up-200bps	This paper	N/A
pGL4.84-Ins2 promoter -up-300bps	This paper	N/A
pGL4.84-Ins2 promoter -up-400bps	This paper	N/A
pGL4.84-Ins2 promoter -up-500bps	This paper	N/A
pGL4.84-Ins2 promoter -up-120bps	This paper	N/A
pGL4.84-Ins2 promoter -up-140bps	This paper	N/A
pGL4.84-Ins2 promoter -up-160bps	This paper	N/A
pGL4.84-Ins2 promoter -up-180bps	This paper	N/A
pGL4.84-Ins2 promoter -up-400bps (A3 del)	This paper	N/A

REAGENT or RESOURCE	SOURCE	IDENTIFIER
Software and algorithms		
ImageJ	NIH	https://imagej.nih.gov/ij/
Prism	GraphPad	https://www.graphpad.com/scientific-software/prism/
Adobe Photoshop	Adobe	https://www.adobe.com/products/photoshop.html
Adobe Illustrator	Adobe	https://www.adobe.com/products/illustrator.html
R studio	R studio	https://rstudio.com/
Other		
Stellaris® RNA FISH Hybridization Buffer	LGC Biosearch tech	#SMF-HB1-10
Stellaris® RNA FISH Wash Buffer A	LGC Biosearch tech	#SMF-WA1-60
Stellaris® RNA FISH Wash Buffer B	LGC Biosearch tech	#SMF-WB1-20
MEM Amino Acids Solution (50X)	Thermo Fisher Scientific	#11130-051
MEM Non-Essential Amino Acids Solution (100X)	Thermo Fisher Scientific	#11140-050
Glucose Solution	Thermo Fisher Scientific	#A24940-01
L-glutamine	Sigma Aldrich	#G7513
Arginine	Sigma Aldrich	A5131
Isoleucine	Sigma Aldrich	I2752
Leucine	Sigma Aldrich	L8912
Valine	Sigma Aldrich	V0513
Dialyzed FBS	Thermo Fisher Scientific	#26400-044
RPMI 1640 Medium Modified w/o L- Glutamine, w/o Amino acids, Glucose	USBiological	#R9010-01
DMEM	Thermo Fisher Scientific	#10566-016
FBS	Biowest	#S162H
Puromycin	Thermo Fisher Scientific	#A1113803